Systems/Circuits

NPY Induces Stress Resilience via Downregulation of I_h in Principal Neurons of Rat Basolateral Amygdala

Heika Silveira Villarroel,[1]* Maria Bompolaki,[2]* James P. Mackay,[1] Ana Pamela Miranda Tapia,[1] Sheldon D. Michaelson,[1] Randy J. Leitermann,[2] Robert A. Marr,[3] Janice H. Urban,[2] and William F. Colmers[1]

[1]Department of Pharmacology, University of Alberta, Edmonton, Alberta, Canada T6G 2H7, [2]Department of Physiology and Biophysics, and [3]Department of Neuroscience, Chicago Medical School, Rosalind Franklin University of Medicine and Science, North Chicago, Illinois 60064

Neuropeptide Y (NPY) expression is tightly linked with the development of stress resilience in rodents and humans. Local NPY injections targeting the basolateral amygdala (BLA) produce long-term behavioral stress resilience in male rats via an unknown mechanism. Previously, we showed that activation of NPY Y_1 receptors hyperpolarizes BLA principal neurons (PNs) through inhibition of the hyperpolarization-activated, depolarizing H-current, I_h. The present studies tested whether NPY treatment induces stress resilience by modulating I_h. NPY (10 pmol) was delivered daily for 5 d bilaterally into the BLA to induce resilience; thereafter, the electrophysiological properties of PNs and the expression of I_h in the BLA were characterized. As reported previously, increases in social interaction (SI) times persisted weeks after completion of NPY administration. *In vitro* intracellular recordings showed that repeated intra-BLA NPY injections resulted in hyperpolarization of BLA PNs at 2 weeks (2W) and 4 weeks (4W) after NPY treatment. At 2W, spontaneous IPSC frequencies were increased, whereas at 4W, resting I_h was markedly reduced and accompanied by decreased levels of HCN1 mRNA and protein expression in BLA. Knock-down of HCN1 channels in the BLA with targeted delivery of lentivirus containing HCN1-shRNA increased SI beginning 2W after injection and induced stress resilience. NPY treatment induced sequential, complementary changes in the inputs to BLA PNs and their postsynaptic properties that reduce excitability, a mechanism that contributes to less anxious behavior. Furthermore, HCN1 knock-down mimicked the increases in SI and stress resilience observed with NPY, indicating the importance of I_h in stress-related behavior.

Key words: CRF; HCN1; lentivirus; neuropeptide Y; shRNA; social interaction

Significance Statement

Resilience improves mental health outcomes in response to adverse situations. Neuropeptide Y (NPY) is associated with decreased stress responses and the expression of resilience in rodents and humans. Single or repeated injections of NPY into the basolateral amygdala (BLA) buffer negative behavioral effects of stress and induce resilience in rats, respectively. Here, we demonstrate that repeated administration of NPY into the BLA unfolds several cellular mechanisms that decrease the activity of pyramidal output neurons. One key mechanism is a reduction in levels of the excitatory ion channel HCN1. Moreover, shRNA knock-down of HCN1 expression in BLA recapitulates some of the actions of NPY and causes potent resilience to stress, indicating that this channel may be a possible target for therapy.

Introduction

The stress response is one of the most important physiological functions present across species, which enables organisms to handle threats to their wellbeing. It is a tightly controlled process engaging cortical and subcortical brain regions to elicit appropriate responses (fight or flight) to identified threats and thus promote survival (Ulrich-Lai and Herman, 2009). Termination of

Received Dec. 14, 2017; revised March 1, 2018; accepted April 5, 2018.

Author contributions: W.F.C. edited the paper. J.P.M., J.H.U., and W.F.C. designed research; H.S.V., M.B., J.P.M., A.P.M.T., S.D.M., R.J.L., R.A.M., J.H.U., and W.F.C. performed research; H.S.V., M.B., J.P.M., A.P.M.T., S.D.M., R.J.L., R.A.M., J.H.U., and W.F.C. analyzed data; H.S.V., M.B., J.P.M., A.P.M.T., S.D.M., J.H.U., and W.F.C. wrote the paper.

This work was supported by the National Institutes of Health (Grants R01MH090297 and R56MH081152 to J.H.U. and W.F.C.) and the Canadian Institutes of Health Research (CIHR Grant MT10520 to W.F.C.). Studentship support came from CIHR (J.P.M.) and Alberta Innovates-Health Solutions (AI-HS) (J.M., S.D.M.) and from the Neuroscience and Mental Health Institute and the Faculty of Medicine and Dentistry, University of Alberta. Kimberly Smith received summer studentship support from AI-HS. W.F.C. is an Alberta Heritage Foundation for Medical Research Medical Scientist. We thank Daniel Johnston at the University of Texas for sharing the HCN1-shRNA and scrambled control constructs; Gina DeJoseph and the Rosalind Franklin University of Medicine and Science Microscopy and Imaging Facility Core for expert technical assistance; Yuetong Li and Ms. Kimberly Smith for assistance with data collection and analysis; and Daniel Johnston, Chung Sub Kim, Quentin Pittman, Marlene Wilson, and J. Amiel Rosenkranz for comments on an earlier version of the manuscript. Some of these results were presented at Society for Neuroscience Annual Meetings (2012–2016).

The authors declare no competing financial interests.

*H.S.V. and M.B. contributed equally to this work.

this "high-alert" response permits reallocation of resources supporting essential activities and behaviors (Joëls and Baram, 2009). Overwhelming stress frequently causes persistent stress responses, resulting in anxiety disorders such as posttraumatic stress disorder (PTSD) (Zuj et al., 2016). Resisting such disorders in the face of intense stress is termed resilience. Understanding more about the mechanisms and circuitry mediating resilience should suggest protective measures for those subjected to high levels of stress. Currently, mechanisms mediating or contributing to the induction and maintenance of resilience are poorly understood (Oken et al., 2015).

Endogenous chemical messengers such as neuropeptide Y (NPY) promote resilience in rodents and humans (Horn et al., 2016). NPY concentrations are decreased in plasma and CSF of soldiers with combat-related PTSD (Rasmusson et al., 2000; Sah et al., 2014) and persons with trauma exposure, depression, and suicide (Ekman et al., 1996; Morgan et al., 2000; Heilig et al., 2004). Conversely, plasma NPY levels are elevated in stress-resilient Special Forces soldiers (Morgan et al., 2000), and correlate with increased coping, resilience, and PTSD remission (Yehuda et al., 2006). Furthermore, individuals with low NPY expression genotypes exhibit higher anxiety scores (Zhou et al., 2008).

NPY mediates anxiolysis in numerous brain regions (Kask et al., 2002), with the basolateral nucleus of the amygdala (BLA) key for NPY's reduction of behavioral stress, mediating stress resilience (Sajdyk et al., 2004, 2008). Acute intra-BLA application of NPY increases social interaction (SI), a well validated measure of anxiety (File and Seth, 2003; Sajdyk et al., 2004, 2008), decreases fear acquisition, and enhances performance in the conflict test (Heilig et al., 1992; Broqua et al., 1995; Gutman et al., 2008). NPY causes acute, dose-dependent hyperpolarization of BLA principal neurons (PNs; comprising both pyramidal and stellate cells) by inhibiting the hyperpolarization-activated, depolarizing H-current (I_h). The H-current is a mixed (Na^+, K^+) conductance that actively depolarizes BLA PNs at rest. The same PNs were depolarized by the anxiogenic neuropeptide corticotropin-releasing factor (CRF), which activated I_h (Giesbrecht et al., 2010). In these neurons, I_h is carried by hyperpolarization-activated, cyclic nucleotide-gated channel subunit 1 (HCN1) (Giesbrecht et al., 2010). In many neurons, I_h is associated with temporal summation of neuronal inputs, neuronal plasticity (Robinson and Siegelbaum, 2003), and affective disorders (Kim et al., 2012). Based on our previous findings (Giesbrecht et al., 2010), I_h is also important in regulating the excitability of the BLA and stress behaviors.

The BLA is central to generating fear responses and emotional regulation (Rainnie et al., 2004, Mirante et al., 2014). Stressful insults increase the excitability of BLA PNs (Vyas et al., 2002, 2006; Padival et al., 2013, Hubert et al., 2014). These stress-related responses are recapitulated by repeated stimulation of BLA CRF receptors, resulting in long-lasting behavioral anxiety correlated with increased neuronal activity and plasticity within the BLA (Rainnie et al., 2004). In contrast, Sajdyk et al. (2008) demonstrated that repeated intra-BLA injections of NPY produce a long-term (2 months) stress resilient behavioral response, an action opposite to that of CRF.

Correspondence should be addressed to Dr. William F. Colmers, Department of Pharmacology and Institute for Neuroscience and Mental Health, University of Alberta, 9-36 MSB, Edmonton, AB T6G 2H7, Canada. E-mail: william.colmers@ualberta.ca.

DOI:10.1523/JNEUROSCI.3528-17.2018

 0270-6474/18/384506-16$15.00/0

Here, we sought to identify mechanisms underlying the establishment of long-term resilience mediated by NPY injections into the BLA and tested the hypothesis that loss of I_h underlies the development of this stress resilience. In animals made stress resilient with NPY (Sajdyk et al., 2008), BLA PNs were hyperpolarized and the magnitude of their I_h was reduced significantly. Furthermore, intra-BLA delivery of shRNA-suppressing rat HCN1 expression resulted in a similar state of behavioral stress resilience. These results suggest that NPY-mediated behavioral stress resilience results at least in part from a reduction in HCN1 expression in BLA PNs.

Materials and Methods

Animals

The care and use of animals was in accordance with protocols approved by the University of Alberta (UA) Animal Care and Use Committee: Health Sciences and Rosalind Franklin University of Medicine and Science (RFUMS) Animal Care and Use Committee, under their respective authorizations. At RFUMS, animals were housed in an Association for Assessment and Accreditation of Laboratory Animal Care International-accredited animal facility. While at UA, they were housed in an alternative animal housing/holding facility approved by the UA Animal Care and Use Committee under authority from the Canadian Council for Animal Care. At both locations, animals were housed in groups of two rats per cage and food and water were supplied *ad libitum*. Animals were kept on a 12:12 light:dark cycle in a room maintained at 23°C. Ambient lighting was ~230 lux.

Stereotaxic surgery procedures

Male Sprague Dawley rats (6–8 weeks old) were obtained from the UA colony and allowed to acclimatize to the laboratory for 3–4 d or rats from Harlan Laboratories were allowed to acclimate to the animal facility at Rosalind Franklin University for 7 d. For all surgical procedures and injection protocols, sterile procedures were followed. Animals were anesthetized with ketamine (90 mg/kg, i.p.) and xylazine (10 mg/kg, i.p.) and placed in a stereotaxic apparatus with a digital readout (David Kopf). Animal body temperature was maintained with a homeothermic monitor (Harvard Apparatus). Bilateral guide cannulae (26 gauge; Plastics One) were implanted stereotaxically to terminate 2.0 mm dorsal to the BLA [anteroposterior (AP): −2.8 mm; mediolateral (ML): ±5.0 mm; dorsoventral (DV): −6.3 mm; Paxinos and Watson, 2013]. Cannulas were secured to the skull with stainless steel screws (0–80× 1/8; Plastics One) and dental cement. After completion of surgery, all animals received intraperitoneal injections of sterile saline (1 ml per animal) and meloxicam (1 mg/kg s.c.) and were placed on a warming pad until fully recovered from the anesthetic. Animals were housed individually for 3 d to recover from the procedure and randomly caged in pairs and kept together throughout the remainder of the experiment.

Intracranial injection procedures

Injections either of NPY (10 pmol/100 nl) or vehicle (Veh; sterile phospate-buffered saline) were delivered bilaterally into the BLA on 5 consecutive days beginning on day 7 after surgery. Two 33 Ga injectors (Plastics One) extending 2 mm beyond the guide cannula were each connected via polyethylene (PE 50) tubing (Plastics One) to a 1 μl syringe (Hamilton) placed in a syringe pump (model PHD 4400; Harvard Instruments). NPY or Veh (100 nl) was delivered per site over 30 s and the injectors remained in place for an additional 2 min. Afterward, the injectors were removed and tested to verify patency. Stylets were replaced into the guide cannulas and animals were returned to their home cage.

HCN1 knock-down

Plasmids and generation of lentivirus. The two plasmids containing HCN1-shRNA and scrambled-shRNA (scr-shRNA), cloned into a pLenti-U6-syn-GFP vector, were generous gifts from Dr. Daniel Johnston (UT-Austin; Kim et al., 2012). Green fluorescent protein (GFP) was included as a marker for transfection. The plasmids were transfected into lentiviral particles with assistance from Dr. Robert Marr (Rosalind

Franklin University) and the University of North Carolina Viral Vector Core.

Stereotaxic microinjections of lentivirus. Stereotaxtic surgery was conducted under sterile conditions using gas anesthesia (4% isoflurane) and following BSL2 guidelines. Two microliters of virus (2×10^9 TU/μl) or Veh (sterile saline) were injected bilaterally over 5 min directly into the BLA (−2.7 mm A/P, ±5 mm M/L, −9 mm V; Paxinos and Watson, 2013) using a neurosyringe (Hamilton). The syringe was maintained *in situ* for another 5 min after the injection before it was removed. Rats were assigned to the following groups: (1) bilateral injection of Veh (saline), (2) lentivirus containing GFP (lenti-GFP), (3) lentivirus containing shRNA with a scrambled sequence (scr-shRNA), or (4) lentivirus containing shRNA with a sequence complimentary to HCN1 mRNA (HCN1-shRNA). Postoperatively, animals were treated with flunixin analgesic (2 mg/kg; Patterson's Veterinarian Supply) for 48 h. To evaluate the degree of knock-down produced by the treatment, animals were anesthetized (4% isoflurane) and decapitated. BLA tissue was removed and protein analysis for HCN1 was performed using Western blotting (below).

Behavioral procedures

Social interaction. Pairs of animals were placed in opposite corners of an open field and SI was recorded on HD video for offline analysis (Sajdyk et al., 2008). SI behavior was initially recorded 3 d before injections ("baseline") and then at 30 min after either NPY or Veh (Veh) injections on days 1 and 5 and weeks 2 and 4. SI was performed at the same time of day (between 0800 and 1300 h). For each SI session, all partner rats were of same sex and similar weight and housed under identical conditions, but had no previous contact with each other. Every SI session for every animal thus involved a unique pair of animals.

HCN1 knock-down. After at least 1 week (1W) of recovery from viral injection surgery, SI experiments were initiated in saline and lentivirus-treated animals, then at 2W, 4W, and 8W by experimenters blinded to treatment. To evaluate the degree of knock-down produced by lentiviral treatment, BLA tissue was removed (4W) as indicated above and Western blot protein analysis for HCN1 performed (below).

Stress resilience. At 4W after lentivirus injections, animals that underwent stress were placed in plastic restrainers for 30 min and SI was determined immediately after the end of the stress session. As a control, animals from the same group that did no undergo stress were placed in transport cages with bedding for 30 min and SI was determined immediately after the end of the no-stress session.

Brain slice preparation

After 2 and 4 weeks from the first injection and at least 1–3 h after the completion of behavioral tests, Veh- or NPY-treated rats were killed by decapitation without prior anesthesia. Brains were carefully but rapidly removed and submerged in cold (<4°C) artificial CSF (ACSF) that contained the following (in mM): 118 NaCl, 3 KCl, 1.3 $MgSO_4$, 1.4 NaH_2PO_4, 5.0 $MgCl_2{\cdot}6H_2O$, 10 glucose, 26 $NaHCO_3$, and 1.5 $CaCl_2$, 300 mOsm bubbled with carbogen (95% O_2, 5% CO_2). Kynurenic acid (1 mM) was added to the slicing solution to prevent damage from ionotropic glutamate receptor activation (Giesbrecht et al., 2010). Coronal brain slices (300 μm) containing the BLA were prepared using a vibrating slicer (Slicer HR2; Sigmann Elektronik). Slices were placed into a room temperature (22°C), carbogenated ACSF solution ("bath solution") containing the following (in mM); 124 NaCl, 3 KCl, 1.3 $MgSO_4$, 1.4 NaH_2PO_4, 10 glucose, 26 $NaHCO_3$, and 2.5 $CaCl_2$, 300 mOsm. Bath solution was used for all remaining experiments. Slices were acclimatized to room temperature for a minimum of 30 min before being placed into the recording chamber. Slices were held submerged by a platinum and polyester fiber "harp" in a fixed-stage recording chamber (Giesbrecht et al., 2010) and viewed with a movable upright microscope (Axioskop FS2; Carl Zeiss). The slices were perfused continuously with warm (34°C ± 0.5°C), carbogenated ACSF between 2 and 2.5 ml/min for ~20 min before any recordings.

Electrophysiology

Pipettes were pulled from thin-walled borosilicate glass (TW150F; World Precision Instruments) with a two-stage puller (PP-83; Narishige). Tip resistance was 5 MΩ when pipettes were filled with an internal solution containing the following (in mM): 5 HEPES, 2 KCl, 136 K^+-gluconate, 5 EGTA, 5 Mg·ATP, and 0.35 GTP. The pH was adjusted to 7.27 with KOH and osmolarity was adjusted to between 285 and 290 mOsm using a micro-osmometer (model 3-MO or 3320; Advanced Instruments). A modified internal solution containing 126 mM Cs^+-methanesulfonate in place of K^+-gluconate was used for certain experiments. In this case, pH was adjusted with CsOH; otherwise, constituents, concentrations, and other properties were identical to the K^+-gluconate internal solution. In most cases, the pipette solution also contained neurobiotin (0.2%) to enable *post hoc* analysis of cell morphology. All recordings were made using either an Axoclamp 2A or a Multiclamp 700B amplifier, data acquired via a Digidata 1322 or Digidata 1440 interface, and experiments controlled and analyzed with pClamp versions 9 or 10 (all Molecular Devices). All membrane potentials reported were corrected for the calculated 15 mV liquid junction potential (Giesbrecht et al., 2010).

The anatomical limits of the BLA were identified based on the atlas of Paxinos and Watson (2013). PNs within the BLA were viewed using infrared-differential interference contrast optics and selected based on morphology and the presence of a large proximal dendrite. Giga-ohm seals were initially established on the soma either in current clamp or voltage clamp; once a seal was formed, the patch was ruptured with the cell held near the resting potential in the voltage-clamp mode. Once whole-cell recording had been established, neurons were routinely held in voltage clamp near rest at −75 mV (corrected for the −15 mV liquid junction potential) except when changes in the resting membrane potential and rheobase were studied in the current-clamp mode. Only cells exhibiting both stable holding current and access resistance for at least 10 min before experimental manipulations were studied further.

Pharmacological studies

Recordings of fundamental neuronal properties, including rheobase, resting membrane potential, action potential parameters, and spontaneous postsynaptic currents were made immediately before drug application (control), during drug application (lasting ~3–4 min), and at regular intervals for 30 min after initiating washout. In some cells, the washout was prolonged and recordings were taken until 45 min after washout began. A similar sequence of recordings, including an assessment of access resistance, was acquired for each cell and condition. Changes in the resting membrane potential were assessed by comparison of continuous (30 s) current-clamp recordings made under each experimental condition in the absence of any imposed current.

Rheobase measurements. To determine rheobase, neurons were held in current clamp near their resting membrane potential (for each condition) and families of between 2 and 8 depolarizing current ramps as needed, were swept linearly from 0 pA to (initially) 100 pA over 800 ms; the peak current was incremented by 100 pA with each successive sweep. The minimum current necessary to elicit the first action potential during a ramp was designated as the cell's rheobase current under the condition studied (see Results).

H currents (I_h). To study I_h, a family of hyperpolarizing voltage steps (−10 mV to −70 mV; Giesbrecht et al., 2010) was applied from a holding potential of −55 mV. The magnitude of I_h at a given potential step was determined as the difference between the initial positive current peak after the capacitative transient and the final, steady-state current for each step (see Fig. 2*A*, inset). Amplitude of I_h was plotted against step potential.

Instantaneous inward rectifying current (I_{ir}). This current was observed as a time-independent inward current seen immediately upon application of a hyperpolarizing voltage step during the H-current protocol. Amplitude of I_{ir} was plotted against step potential. For clarity, mean net I_{ir} is plotted as net current lost with NPY treatment.

Histology. In most cases, neurons were filled with neurobiotin via the pipette during the recording, fixed overnight in 4% buffered formalin, and then retained for *post hoc* morphological studies at a later time.

Chemicals and drugs. For slicing, bath and pipette solutions, kynurenic acid was obtained from Abcam; Mg^{2+} ATP, NaH_2PO_4, $CaCl_2{\cdot}2H_2O$, K^+-gluconate, Cs^+-methansulfonate, and CsOH were obtained from Sigma-Aldrich, and Na-GTP was obtained from Roche Diagnostics. All

remaining chemicals were obtained from Fisher Scientific. NPY (rat/human) was obtained from either Peptidec Technologies or PolyPeptide Laboratories; CRF was obtained from Phoenix Pharmaceuticals. All peptides were dissolved in HPLC-grade water (Fisher Scientific or Sigma-Aldrich) and then stored at −20°C as individual aliquots of at least 100-fold the applied concentration until immediately before use. Neurobiotin was obtained from Vector Laboratories.

qRT-PCR

Two or 4 weeks after the NPY treatment, animals were anesthetized with isoflurane and decapitated. Brains were removed and BLA tissue was isolated by dissection with the aid of a dissecting microscope from 1-mm-thick sections prepared using a stainless steel brain matrix (Ted Pella). BLA tissue was placed in RNase-free microcentrifuge tubes, quickly frozen on dry ice, and stored in at −80°C until processing for mRNA extraction. During dissection, cannula placements were verified and noted. Tissues with cannula placements that missed BLA were removed from analysis.

Tissue was homogenized and mRNA was isolated using Qiagen Mini RNAeasy kits. cDNA was generated using High-Capacity cDNA Reverse Transcription kits. Aliquots (12–15 ng) of cDNA were subjected to real time qRT-PCR using TaqMan probes for the HCN1–4, CRFR1 and 2, and NPY Y_1 and Y_2 receptors. The various primers sets were multiplexed with hypoxanthine-guanine phosophoribosyltransferase (HPRT) as the internal control. Samples were assayed in triplicate with HPRT included in the multiplex reaction. Resultant DNA products were quantified using ΔΔCT method (Livak and Schmittgen, 2001). Each data value represents the targeted sequence mRNA normalized to HPRT; data are represented as fold change from 2W Veh control group. Data are presented as mean ±SEM. Statistical analysis was performed using a two-way ANOVA and Bonferroni post test.

Western blotting

2W or 4W after the NPY treatment, animals were anesthetized with isoflurane and decapitated. Brains were removed and BLA tissue was isolated as described above for qRT-PCR. Total protein was extracted using radioimmunoprecipitation assay buffer containing a mixture of proteinase inhibitors (Pierce) and concentrations were determined using a Bradford-based assay (Pierce). Proteins (10 μg) were subjected to PAGE on a gradient 8–16% Tris-Glycine gel (Novex) and transferred to PVDF membranes (Bio-Rad). Membranes were incubated in blocking solution (5% milk in 0.1 M TBS and 0.1% Tween 20; TBST) for 1 h at room temperature before being transferred to a solution containing primary antibody diluted in blocking solution overnight at 4°C. The primary antibodies used were guinea pig guinea pig anti-HCN1 (1:2000; Alomone Laboratories, catalog #AGP-203), rabbit anti-HCN2 (1:1000; Alomone Laboratories, catalog #APC-030, RRID:AB_2313726), rabbit anti-HCN4 (1:2000; Alomone Laboratories, catalog #AGP-004, RRID:AB_2340957), mouse anti-TRIP8b exon4 (1:10,000; UC Davis/NIH NeuroMab Facility, catalog #73–208, RRID:AB_2162409), and mouse anti-βActin (1:20,000, Sigma-Aldrich, catalog #A5441, RRID:AB_476744). Membranes were washed in TBST 4 × 20 min before incubation in HRP-conjugated secondary antibody [1:15,000 (HCN1; HCN2; HCN4) and 1:20,000 (β-actin; TRIP8b)]. The HRP-conjugated secondary antibodies used were goat anti-guinea pig (Thermo Fisher Scientific, catalog #A18769, RRID:AB_2535546), anti-rabbit (GE Healthcare Life Sciences, catalog #NA934v), and anti-mouse (GE Healthcare Life Sciences, catalog #NA931v). Membranes were washed again in TBST 4 × 20 min. Protein bands were visualized using chemiluminescence (Pierce SuperSignal West Dura and Pico Substrate) and the blots were apposed to film (Kodak). Films were scanned and images analyzed with ImageJ software. Data were analyzed in triplicate and normalized to actin control; they are reported as the fold change from the appropriate control group (2W or scrambled control).

Immunohistochemistry

Immunohistochemistry was performed on tissue obtained from animals injected with lentivirus expressing HCN1-shRNA. Rats were anesthetized (pentobarbital, 50 mg/kg, i.p.) and transcardially perfused with 4% paraformaldehyde. Brains were removed, postfixed overnight at 4°C, and tissues were sectioned on a vibratome (40 μm); free floating sections were processed as described previously (Giesbrecht et al., 2010). Tissues were labeled for the HCN1 subunit (mouse anti-HCN1; 0.5 μg/ml; UC Davis/NIH NeuroMab Facility, catalog #75-110, RRID:AB_2115181) and signal was visualized using biotinylated tyramide protocol with Alexa Fluor 594 streptavidin (1:250, Invitrogen, catalog #S11227). Sections were mounted on on Superfrost charged glass slides and coverslips were applied using PVA-DABCO (polyvinyl alcohol; 1,4 diazabicyclo [2.2.2]octane). Immunoreactivity was observed using an Olympus Fluoview Confocal microscope (Microscopy and Imaging Facility; Rosalind Franklin University). GFP (green) signal was used as a marker for viral transfection and injection placements. Images were scanned and imported and brightness and contrast were adjusted.

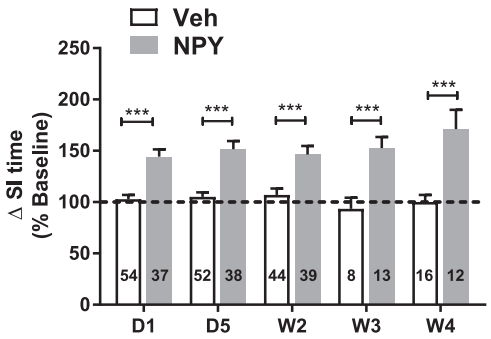

Figure 1. SI times increase with repeated NPY injections into BLA. SI for animals injected bilaterally with NPY (10 pmol/100 nL) or Veh into the BLA daily for 5 d (D1–D5) was measured at times indicated. SI is presented relative to preinjection baseline values for each individual animal (linear mixed-model; treatment: $F_{(1,100.6)} = 54.0$, $p < 0.0001$; time: $F_{(4,44.7)} = 0.611$, $p = 0.657$; interaction: $F_{(4,44.7)} = 1.42$, $p = 0.24$). Numbers of animals tested are indicated in each column. ***$p < 0.001$, Bonferroni's multiple-comparisons test.

Experimental design and statistical analysis

Data are represented as means ± SEM. All data were analyzed using GraphPad Prism software (versions 6 and 7) or SSPS (version 20). The D'Agostino-Pearson omnibus normality test was applied to determine data distribution. Although no power analyses were performed, sample sizes were determined based on previously reported studies. For the analysis of behavioral, gene, and protein expression data with a Gaussian distribution, a two-way ANOVA was used, whereas for data with multiple time points, a two-way repeated-measures (RM) ANOVA was used, followed by a Bonferroni *post hoc* test if the ANOVA indicated significance. For SI studies with NPY, a linear mixed-model with repeated measures (to account for missing data points associated with repeated measures) with an autoregressive-heterogenous covariance matrix and using maximum likelihood method for estimations was used. As fixed effects, we entered treatment and time (with interaction term); we used intercepts for subjects as random effects. For electrophysiological studies, comparisons were made between neurons from Veh- and NPY-treated animals at matched postinjection times by unpaired *t* tests for two means with a normal distribution; effects of drug applications were analyzed by paired *t* tests with a normal distribution. Current–voltage (*I–V*) relationships were analyzed using two-way RM ANOVA with Bonferroni *post hoc* tests for significance at individual potentials. The numbers of neurons recorded, along with the numbers of animals per group, are indicated in the text and/or figure legends. Complete statistical analyses are provided in the figure legends.

Results

NPY treatment results in a durable anxiolytic phenotype

Repeated injections of NPY into the BLA produced long-term increases in SI relative to Veh at all times tested and as described previously (Sajdyk et al., 2008). NPY-treated animals had significant increases in SI relative to Veh-treated groups at all times tested. (Fig. 1). Increases in SI are consistent with a less anxious

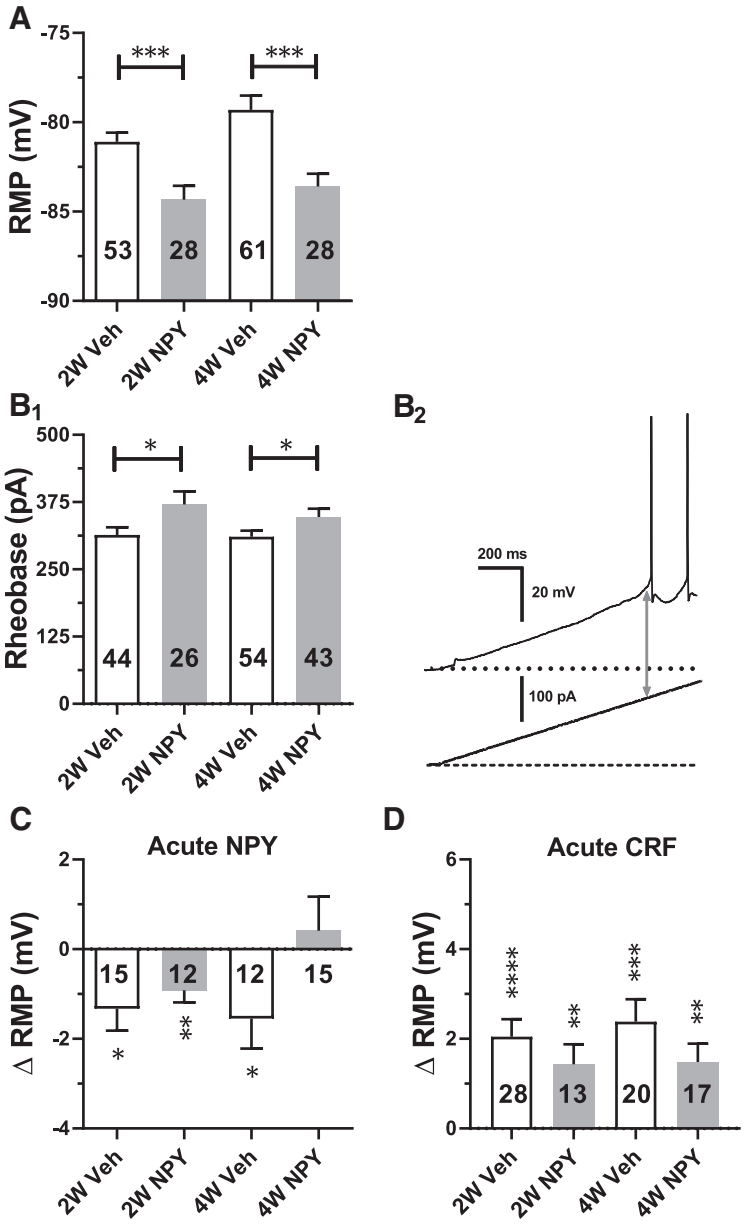

Figure 2. Effects of repeated NPY or Veh treatment on electrophysiological properties of BLA PNs in brain slices taken at 2W and 4W after initiation of treatment. Data are represented as mean ± SEM. Numbers of individual neurons tested are indicated in each bar. ***A***, Effect on resting membrane potential (RMP; 2W: $t_{(79)} = 3.57$, $p = 0.0006$; NPY: $n = 28$ cells/24 rats, Veh: $n = 53/17$ and 4W: $t_{(107)} = 3.86$, $p = 0.0002$, NPY: $n = 61/30$ Veh: $n = 48/22$). ***B1***, Effect on rheobase (2W: $t_{(68)} = 2.16$, $p = 0.034$; NPY: $n = 26/16$ Veh: $n = 44/25$ and 4W: $t_{(95)} = 1.98$, $p = 0.04$; NPY: $n = 43/22$, Veh: $n = 54/32$). ***B2***, Representative current-clamp recording depicting rheobase measurement as magnitude of ramp current (arrow) required to induce action potential firing from rest in a 2W Veh-treated neuron. ***C***, Effect of acute NPY (1 μM) application on RMP as indicated (2W-Veh: $t_{(14)} = 2.73$, $p = 0.016$; 2W-NPY: $t_{(11)} = 3.44$, $p = 0.0055$; 4W-Veh: $t_{(11)} = 2.30$, $p = 0.042$, 4W-NPY: $t_{(14)} = 0.54$, $p = 0.60$). Data from 12 rats in each group are shown (ANOVA with Bonferroni's multiple-comparisons test $F_{(3,50)} = 2.30$, $p = 0.089$). ***D***, Effect of acute CRF (30 nM) application on RMP as indicated (2W-Veh: $t_{(27)} = 5.30$, $p = 1.35e\text{-}5$; 2W-NPY: $t_{(12)} = 3.20$, $p = 0.0076$; 4W-Veh: $t_{(19)} = 4.77$, $p = 0.0001$, 4W-NPY: $t_{(16)} = 3.595$, $p = 0.0024$). Data from 9–17 rats in each group are shown (ANOVA with Bonferroni's multiple-comparisons test $F_{(3,74)} = 0.96$, $p = 0.42$). ***A***, ***B***, Unpaired *t* tests; ***C***, ***D***, paired-*t* tests. $^*p < 0.05$, $^{**}p < 0.01$, $^{***}p < 0.001$, $^{****}p < 0.0001$.

behavioral phenotype, which persisted long after the end of peptide administration (2–8 weeks; Sajdyk et al., 2008).

NPY treatment decreases principal cell excitability in *ex vivo* brain slices

The acute anxiolytic action of NPY in the BLA correlates with hyperpolarization and decreases in the excitability of BLA pyramidal cells caused by the inhibition of a resting I_h (Giesbrecht et al., 2010). We therefore hypothesized that the prolonged increase in SI caused by repeated NPY treatment in the BLA would correlate with a long-term decrease in the excitability of BLA PNs (Sajdyk et al., 2008). Therefore, in recordings from acute BLA slices taken from NPY-treated animals 2W and 4W after injections, PNs were hyperpolarized at rest at both time points compared with those from Veh-treated animals (Fig. 2*A*).

The hyperpolarization seen with acute NPY treatment of naive BLA PNs was accompanied by an increase in the rheobase current when measured from the (hyperpolarized) resting potential (Giesbrecht et al., 2010). Rheobase current from rest was also significantly increased in PNs from NPY-treated animals (2W and 4W), which were hyperpolarized compared with those from Veh-treated animals (Fig. 2*B*), consistent with a chronic reduction in PN excitability after repeated NPY treatment.

To determine the effect of repeated NPY treatment on the resting input resistance of BLA PNs, cells from 4W Veh- or NPY-injected animals received a single hyperpolarizing current clamp step (50 or 100 pA) from the resting potential. Input resistance of neurons from 4W NPY-treated animals was 72.3 ± 6.2 MΩ (n = 17cells/12 animals) versus 79.2 ± 6.0 MΩ (n = 19/11) in 4W Veh-treated animals ($t_{(34)} = 0.799$, $p = 0.43$; data not shown), meaning that input resistance near rest was unchanged despite the hyperpolarization seen in BLA neurons from NPY-treated animals.

To determine whether BLA neurons from 2W and 4W NPY-treated rats still responded acutely to application of NPY or CRF (Giesbrecht et al., 2010), we treated neurons from Veh- or NPY-treated animals with acute bath applications of either NPY (1 μM) or CRF (30 nM). Application of NPY acutely induced a small yet significant hyperpolarization in PNs both from Veh-treated (2W and 4W) and NPY-treated (2W) animals, but not in PNs from 4W NPY-treated animals (Fig. 2*C*; $p = 0.60$). In contrast, CRF application depolarized neurons from all treatment groups (Fig. 2*D*).

NPY treatment reduces resting I_h amplitude in BLA PNs

Acute NPY application decreases BLA PN excitability by reducing resting I_h (Giesbrecht et al., 2010). Therefore, we assessed the effect of repeated NPY injections on I_h in voltage-clamp recordings from BLA PNs 2W and 4W after treatment. There were no significant differences between I_h amplitudes in BLA PNs from 2W Veh- and NPY-treated animals at any potential tested

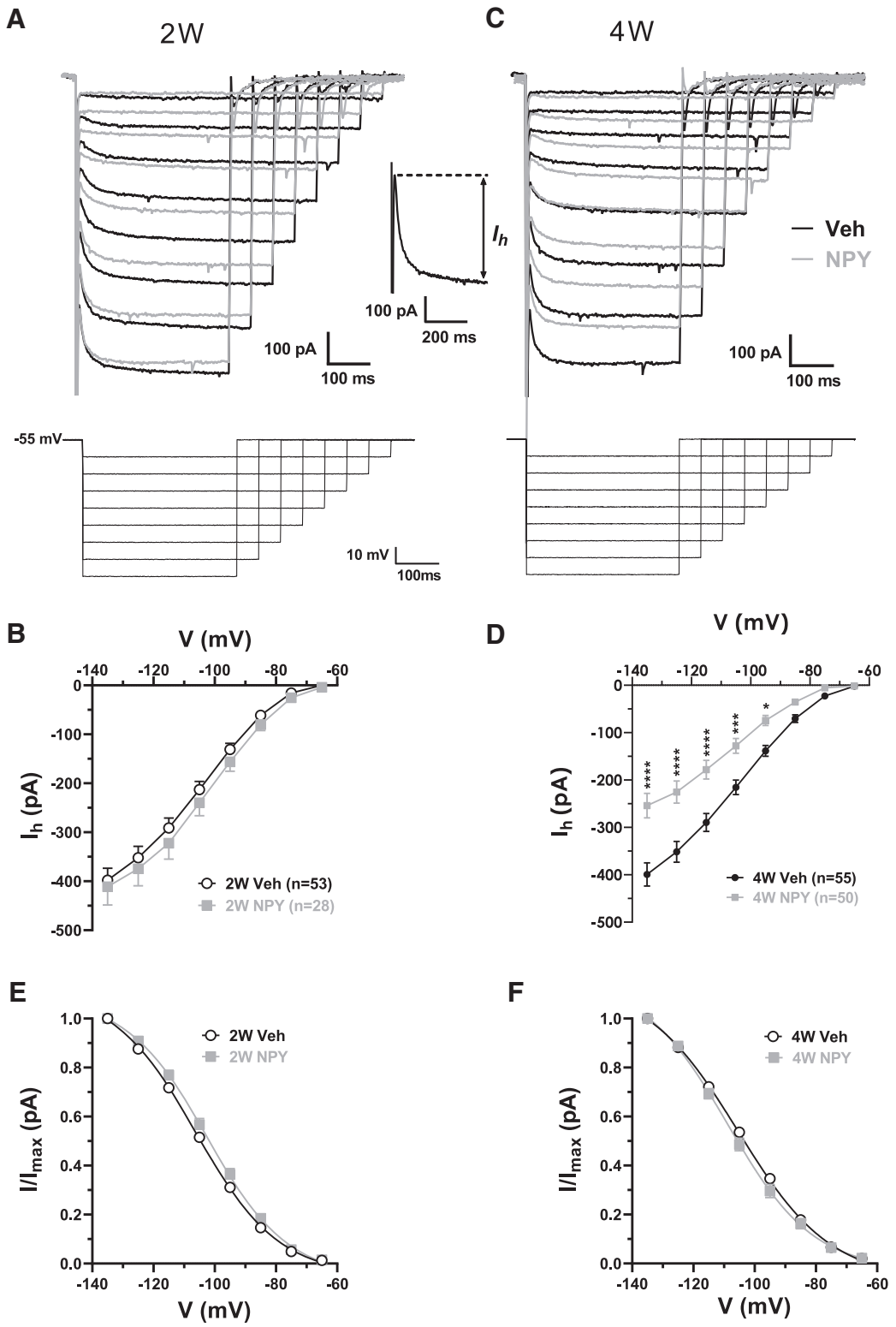

Figure 3. Repeated NPY treatment diminishes resting I_h in BLA PNs. ***A***, Top, Superimposed current responses to families of hyperpolarizing voltage clamp steps (bottom) from $V_h = -55$ mV from a representative Veh-treated (black traces) and NPY-treated (gray traces) neuron 2W after the first injection. Inset, Illustration of I_h measurement (response to a step to −135 mV). ***B***, *I–V* relationship of I_h from neurons (numbers as indicated) from 2W Veh-treated (white circles) and NPY-treated (gray squares) rats. Data from 25 and 16 rats, respectively, are shown; cell numbers are as indicated (2-way RM-ANOVA: treatment: $F_{(1,78)} = 0.645$, $p = 0.42$; voltage: $F_{(7,546)} = 334.9$, $p < 0.0001$; interaction: $F_{(7,546)} = 0.292$, $p = 0.96$. ***C***, Top, Superimposed current traces to voltage steps (bottom) as in ***A*** for representative neurons from animals 4W after treatment with Veh (black traces) or NPY (gray traces). ***D***, *I–V* relationship of I_h from 4W Veh- (white circles) and NPY-treated animals (gray squares) (Veh $n = 55$ cells/34 rats, NPY $n = 50/20$; 2-way RM-ANOVA: treatment: $F_{(1,104)} = 17.67$, $p < 0.0001$; voltage: $F_{(7,728)} = 285.9$, $p < 0.0001$; interaction: $F_{(7,728)} = 12.78$, $p < 0.0001$. Bonferroni's multiple-comparisons test; ***C***,***D***). ***E***, ***F***, Fractional activation of I_h versus step potential for neurons from 2W (***E***) and 4W (***F***) Veh- and NPY-treated animals. Boltzmann fits and corresponding midactivation voltages ($V_{1/2}$) indicated no significant differences in fractional activation between neurons from Veh- and NPY-treated animals (2W: Veh: -105.4 ± 1.1 mV, $n = 48$ neurons from 25 rats; NPY: -102.0 ± 1.4 mV, $n = 24$ neurons from 16 rats; unpaired *t* test: $t_{(70)} = 1.81$, $p = 0.075$; 4W: Veh: -103.3 ± 1.3 mV, $n = 49$ neurons from 34 rats; NPY: -105.9 ± 1.6 mV, $n = 38$ neurons from 20 rats; unpaired *t* test: $t_{(85)} = 1.25$, $p = 0.22$). In ***B*** and ***D–F***, numbers of individual neurons/rats tested are as indicated in legends. Data in ***B–F*** are represented as mean ± SEM. $^*p < 0.05$, $^{**}p < 0.01$, $^{***}p < 0.001$, $^{****}p < 0.0001$, Bonferroni's multiple-comparisons test or *t* test where appropriate.

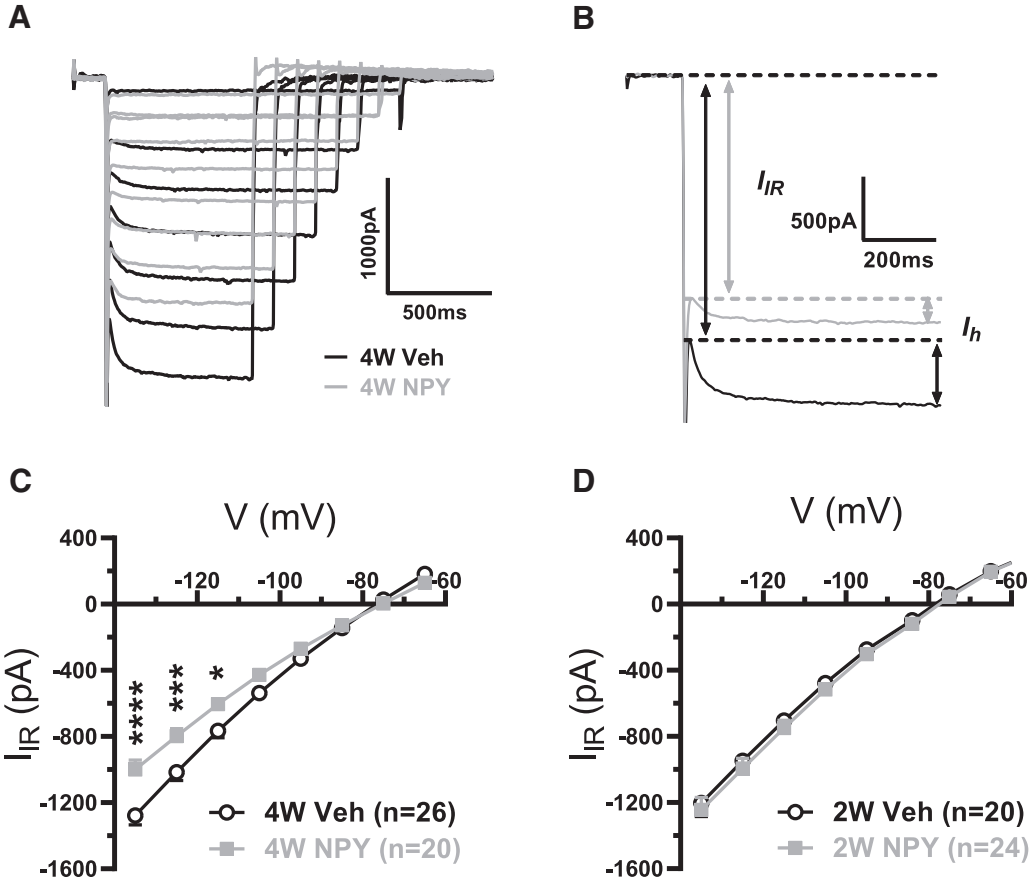

Figure 4. I_{ir} current in BLA PNs is diminished by repeated NPY treatment at 4W. ***A***, Superimposed voltage-clamp current traces from representative 4W Veh-treated (black traces) and NPY-treated (gray traces) neurons as in Figure 2. ***B***, Illustration of I_{ir} and I_h measurement from traces in *A* (step to −135 mV from V_h = −55 mV). ***C***, *I–V* relationship of I_{ir} from BLA neurons from 4W Veh- and NPY-treated animals. Data (mean ± SEM) are shown from 14 and 18 rats, respectively (2-way RM-ANOVA; treatment: $F_{(1,44)} = 5.334$, $p = 0.026$; voltage: $F_{(7,308)} = 853.6$, $p < 0.0001$; interaction: $F_{(7,308)} = 14.24$, $p < 0.0001$). ***D***, *I–V* relationship of I_{ir} from BLA neurons from 2W Veh-treated (white circles) and NPY-treated (gray squares) animals. Data (mean ± SEM) are from 10 and 14 rats, respectively (2-way RM-ANOVA; treatment: $F_{(1,42)} = 0.38$, $p = 0.54$; voltage: $F_{(8,336)} = 531.5$, $p < 0.0001$; interaction: $F_{(8,336)} = 0.137$, $p = 0.998$). *$p < 0.05$, **$p < 0.01$, ***$p < 0.001$, ****$p < 0.0001$, Bonferroni's multiple-comparisons test.

(Fig. 3*A*,*B*). In contrast, at 4W, at voltages negative to −85 mV, I_h was significantly smaller in NPY- than in Veh-treated PNs (Fig. 3*C*,*D*). The half-maximal voltage of I_h activation was not affected by NPY treatment (Fig. 3*E*,*F*). Therefore, 4W after repeated NPY treatment, BLA PNs lost >35% of their maximal I_h, with no change in activation kinetics.

NPY treatment decreases an inwardly rectifying current

Sosulina et al. (2008) reported the acute activation of an inwardly rectifying K^+ conductance by NPY in LA PNs. During the above studies of I_h in the BLA, another current was seen to precede I_h during a hyperpolarizing voltage step (Fig. 4*A*,*B*; Doupnik et al., 1995). At 4W, the magnitude of this I_{ir} current was significantly reduced in neurons from NPY- versus Veh-treated BLA (Fig. 4*C*), but was not different at 2W (Fig. 4*D*). The I_{ir} lost with repeated NPY treatment had an apparent reversal potential at ∼−80 mV (data not shown).

NPY treatment reduces I_h responses to acute NPY and CRF application

The acute inhibitory and excitatory actions of NPY and CRF on BLA PNs have been attributed to the inhibition and enhancement of resting I_h, respectively (Giesbrecht et al., 2010). In cells from 2W and 4W Veh-treated animals, acute application of NPY (1 μM) to BLA PNs held in voltage clamp resulted in the inhibition of I_h (Fig. 5), which is consistent with earlier findings (Giesbrecht et al., 2010). Specifically, I_h was significantly reduced by NPY at all potentials negative to −85 mV at 2W (Fig. 5*A*) and at all potentials negative to −75 mV at 4W (Fig. 5*B*). However, I_h was insensitive to acute NPY application in PNs from NPY-treated animals at 2W and only very slightly sensitive at 4W (Fig. 5*C*,*D*), suggesting a reduction in Y_1 receptor expression or coupling in response to repeated NPY treatment (Giesbrecht et al., 2010).

In BLA neurons from Veh-treated animals, acute application of CRF (30 nM) enhanced I_h relative to control at potentials negative to −85 mV (Fig. 6*A*) and at potentials negative to −95 mV (Fig. 6*B*) for 2W and 4W Veh-treated animals, respectively. However, in BLA neurons from NPY-treated animals, I_h was not affected by CRF (Fig. 6*C*,*D*). The results suggest that the sensitivity of I_h to acute application either of NPY or CRF is already diminished or abolished at 2W in NPY-treated BLA PNs, followed by a significant loss of resting I_h at 4W.

NPY treatment affects spontaneous synaptic events in BLA PNs

Amygdala neurons receive greater excitatory synaptic input after repeated stress exposure (Padival et al., 2013) or after repeated subacute injections of the CRFR agonist urocortin, which nonetheless induce anxiety-like behaviors after 5 successive days of treatment (Rainnie et al., 2004). At 2W after repeated NPY treat-

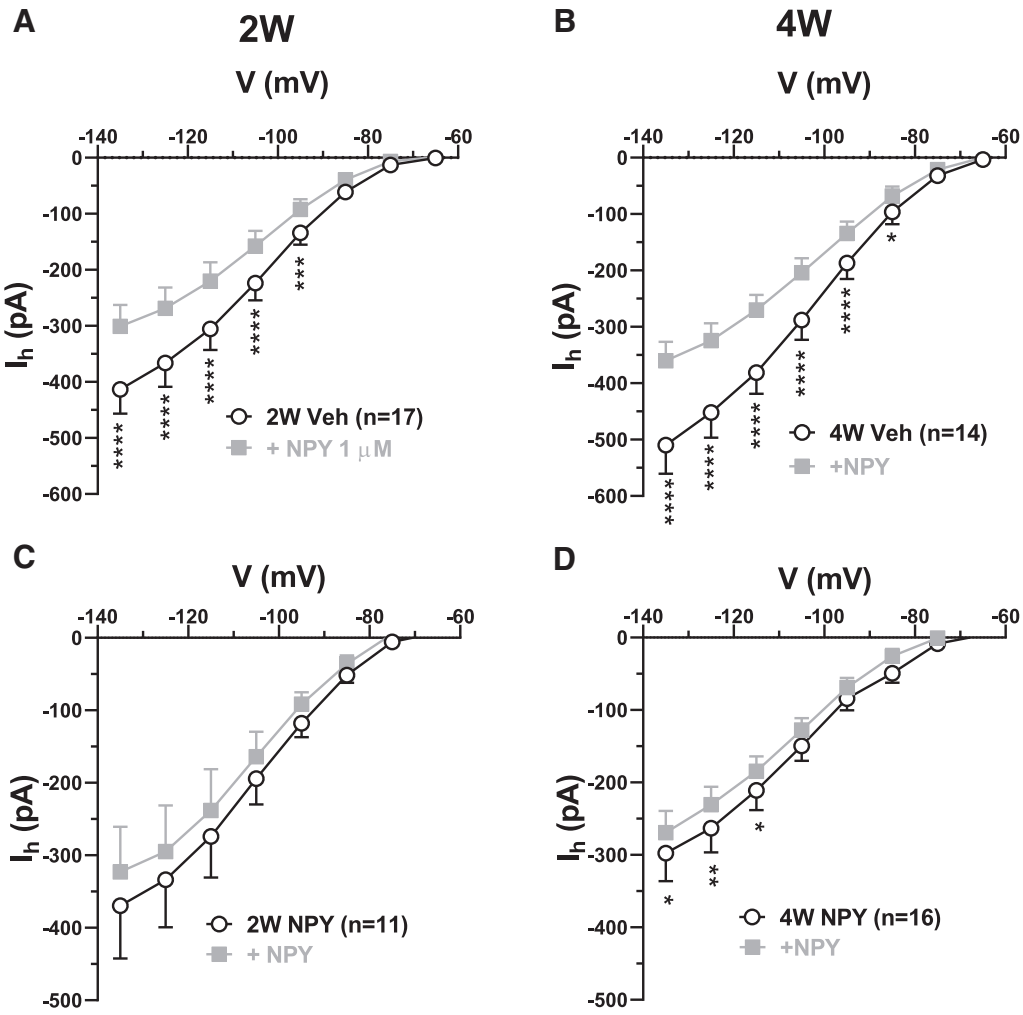

Figure 5. Acute effect of NPY on I_h is reduced in 2W and 4W NPY-treated BLA PNs. ***A***, *I–V* relationship for I_h in the absence (○) and presence of 1 μM NPY (■) in slices from 2W Veh-treated BLA. (2-way RM-ANOVA; treatment: $F_{(1,16)} = 16.04$, $p = 0.001$; voltage: $F_{(7,112)} = 74.99$, $p < 0.0001$; interaction: $F_{(7,112)} = 19.77$, $p < 0.0001$; $n = 17/12$ rats). ***B***, *I–V* relationship for I_h as in *A* for neurons in slices from 4W Veh-treated BLA (2-way RM-ANOVA; treatment: $F_{(1,13)} = 25.22$, $p = 0.0002$; voltage: $F_{(7,91)} = 102.8$, $p < 0.0001$; interaction: $F_{(7,91)} = 33.42$, $p < 0.0001$; $n = 14/10$ rats). ***C***, *I–V* relationship for I_h of BLA PNs from 2W NPY-treated animals (2-way RM-ANOVA; treatment: $F_{(1,10)} = 4.49$, $p = 0.06$; voltage: $F_{(7,70)} = 22.82$, $p < 0.0001$; interaction: $F_{(7,70)} = 2.03$, $p = 0.063$, $n = 11/11$ rats). ***D***, *I–V* relationship for I_h for neurons in slices from 4W NPY-treated BLA. (2-way RM-ANOVA; treatment: $F_{(1,15)} = 5.936$, $p = 0.028$; voltage: $F_{(7,105)} = 54.08$, $p < 0.0001$; interaction: $F_{(7,105)} = 1.503$, $p = 0.17$, $n = 16/12$ rats). Numbers of neurons are indicated; only neurons with responses to peptide application that reversed on washout were included. $^*p < 0.05$, $^{**}p < 0.01$, $^{***}p < 0.001$, $^{****}p < 0.0001$, Bonferroni's multiple-comparisons test.

ment, BLA PNs were already hyperpolarized, although I_h was unaffected, so we hypothesized that NPY treatment might increase synaptic inhibition at this time point. We simultaneously recorded sIPSC (outward current) or sEPSC (inward current) activity in BLA PNs from 2W NPY- or Veh-treated animals held in voltage clamp at −55 mV using the K^+ gluconate pipette solution. Under these conditions, we observed no significant effect of treatment on either frequency or amplitude for sIPSCs (data not shown).

An earlier study (Smith and Dudek, 1996) indicated higher sIPSC frequencies in BLA PNs than we observed in the above experiments. To clarify this, we increased the resolution of our sIPSC recordings by recording from 2W BLA PNs using a Cs^+ gluconate pipette solution, permitting us to hold them in voltage clamp at −15 mV. Such recordings revealed much higher sIPSC frequencies than were seen at −55 mV (Fig. 7*A*). sIPSC interevent intervals (IEIs) were relatively smaller in cells from 2W NPY-treated compared with 2W Veh-treated animals; sIPSC amplitudes did not differ between treatment groups (Fig. 7*B*). Similarly, sIPSC IEIs were lower in 4W NPY- versus 4W Veh-treated PNs (Fig. 7*C*). Therefore, NPY treatment also induced a pronounced increase in sIPSC frequencies both at 2W and at 4W.

Recordings made at −15 mV with intracellular Cs^+ did not permit analysis of sEPSCs. However, reanalysis of the recordings made with internal K^+ at 2W revealed a modest but significant decrease in sEPSC frequency, accompanied by an modest but significant increase in sEPSC amplitude (Fig. 7*D*). Similar analysis of sEPSC data at 4W did not indicate any differences between Veh and NPY-treated BLA neurons (IEI: $t_{(20)} = 1.422$, $p = 0.1887$; amplitude: $t_{(20)} = 1.827$, $p = 0.894$; $n = 11/10$ rats each, unpaired *t* test, data not shown). Therefore, NPY may effect modest changes in sEPSCs at 2W, but not at 4W.

NPY decreases HCN1 subunit expression

Repeated injections of NPY into the BLA decreased the responsiveness of I_h in BLA neurons to both NPY and CRF at 2W and significantly attenuated I_h at 4W after injection. To determine the mechanism underlying the development of these changes, qRT-PCR was used to evaluate the expression of mRNA-encoding HCN channels and NPY and CRF receptors in the BLA of Veh-

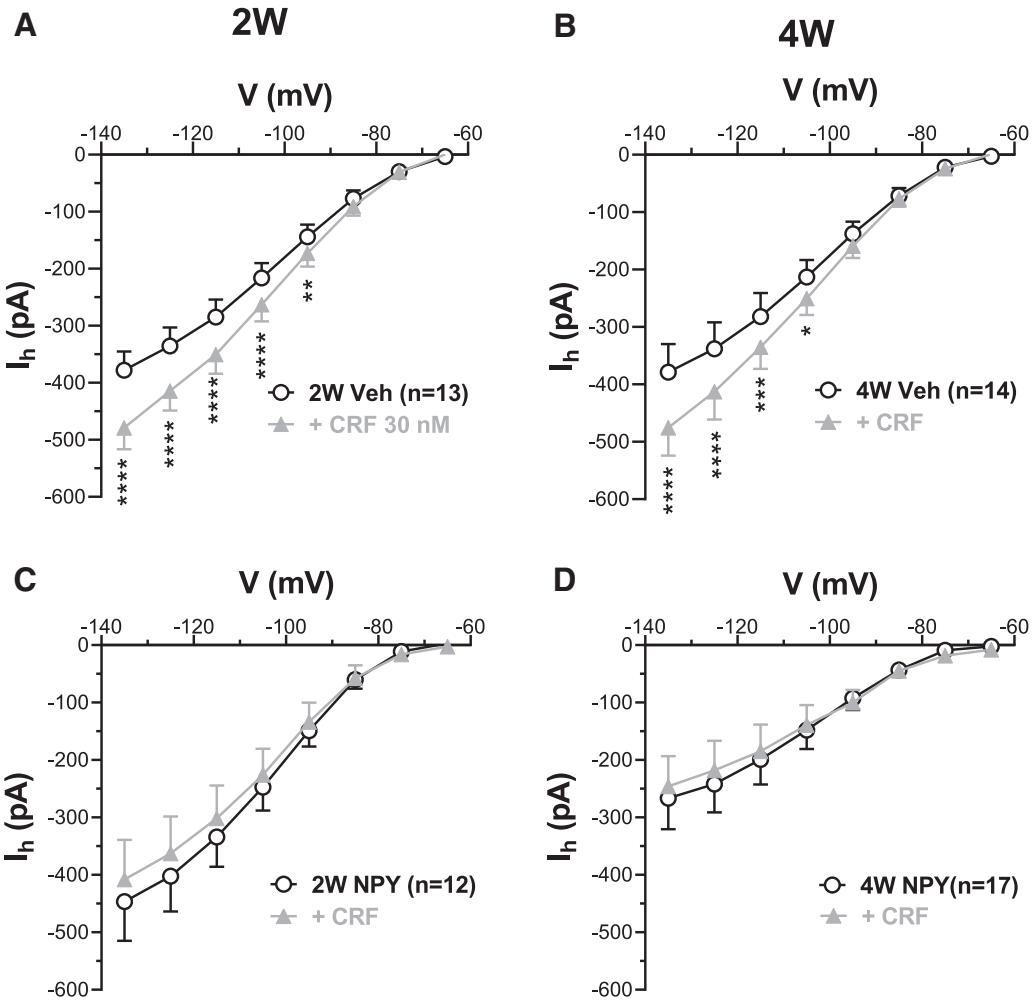

Figure 6. Acute effect of CRF on I_h is reduced in 2W and 4W NPY-treated BLA PNs. ***A***, *I–V* relationship for I_h in the absence (white circles) and presence of 30 nM CRF (gray triangles) in slices from 2W Veh-treated BLA (2-way RM-ANOVA; treatment: $F_{(1,12)} = 37.36, p < 0.0001$; voltage: $F_{(7,84)} = 142.1, p < 0.0001$; interaction: $F_{(7,84)} = 23.46, p < 0.0001$; $n = 13/10$ rats). ***B***, *I–V* relationship for I_h as in ***A*** for neurons in slices from 4W Veh-treated BLA (2-way RM-ANOVA; treatment: $F_{(1,13)} = 11.97, p = 0.0042$; voltage: $F_{(7,91)} = 68.08, p < 0.0001$; interaction: $F_{(7,91)} = 9.73, p < 0.0001$; $n = 14/11$ rats). ***C***, *I–V* relationship for I_h for neurons in slices from 2W NPY-treated BLA (2-way RM-ANOVA; treatment: $F_{(1,11)} = 2.18, p = 0.17$; voltage: $F_{(7,77)} = 38.93, p < 0.0001$; interaction: $F_{(7,77)} = 2.32, p = 0.033$; $n = 12/10$ rats). ***D***, *I–V* relationship for I_h for neurons in slices from 4W NPY-treated BLA (2-way RM-ANOVA; treatment: $F_{(1,16)} = 0.35, p = 0.56$; voltage: $F_{(7,112)} = 19.56$, $p < 0.0001$; interaction: $F_{(7,112)} = 3.35$, $p = 0.0028$; $n = 17/13$ rats). Numbers of neurons tested are indicated. *$p < 0.05$, **$p < 0.01$, ***$p < 0.001$, ****$p < 0.0001$, Bonferroni's multiple-comparisons test.

and NPY-treated animals at 2W and 4W after treatment. Behavioral studies validated the efficacy of NPY treatment seen as increased SI in these animals (Veh: 106.3 ± 7.6 s; NPY: 173.3 ± 12.7 s; $n = 8$ rats each, $t_{(14)} = 4.53$, $p = 0.0005$; Student's unpaired *t* test, data not shown).

qRT-PCR studies on tissue from naive animals indicated that HCN1 and HCN2 subunit mRNAs were more abundant within the BLA than mRNAs encoding HCN3 and HCN4. Quantitation of mRNA samples from 2W and 4W tissue revealed significant decreases in HCN1 gene expression in 4W NPY- versus Veh-treated rats (Fig. 8*A*; $p = 0.04$). HCN2 and HCN3 gene expression remained unchanged compared with Veh (Fig. 8*B*,*C*), but HCN4 subunit expression was increased at 4W both in Veh and NPY treatment groups (Fig. 8*D*; $p = 0.018$ and $p = 0.016$ respectively). Due to the low abundance of HCN4 mRNA in the BLA, the physiological relevance of this change needs to be explored further.

Corresponding to the decrease in HCN1 mRNA levels, NPY treatment also resulted in a ~19% decrease in BLA HCN1 protein levels as determined by Western analysis (Fig. 9*A*), whereas HCN2 (2W Veh: 1.01 ± 0.079; 2W NPY: 1.058 ± 0.098; 4W veh: 0.980 ± 0.064; 4W NPY: 1.088 ± 0.066 relative protein expression from 2W Veh group) and HCN4 (2W Veh: 0.988 ± 0.047; 2W NPY: 1.081 ± 0.121; 4W veh: 0.936 ± 0.116; 4W NPY: 0.801 ± 0.044 relative protein expression from 2W Veh group) protein was not altered either by time or treatment (HCN2: two-way ANOVA: treatment: $F_{(1,25)} = 0.09826$; $p = 0.3310$; time: $F_{(1,25)} = 2.32e\text{-}009$; $p = 0.9999$; interaction: $F_{(1,25)} = 0.1441$;$p = 0.7075$ and HCN4: two-way ANOVA: treatment: $F_{(1,20)} = 0.06151$; $p = 0.8067$; time: $F_{(1,20)} = 3.858$; $p = 0.0636$; interaction: $F_{(1,20)} = 1.825$;$p = 0.1919$). Trafficking and insertion of HCN channel subunits to the plasma membrane is facilitated by the TRIP8b family of proteins (Lewis et al., 2009). TRIP8b protein expression was decreased significantly in the BLA of the same 2W NPY-treated animals; levels returned to those of Veh-treated controls at 4W (Fig. 9*B*; $p = 0.025$).

Repeated NPY treatment did not alter the expression of NPY Y_1 receptor (Y_1R) mRNA at the 2W and 4W time points (Fig. 10*A*). Y_2R mRNA expression was significantly decreased at 4W with NPY treatment (Fig. 10*B*). Levels of CRFR1 and CRFR2 receptor gene expression were not affected either by treatment or time (Fig. 10*C*,*D*).

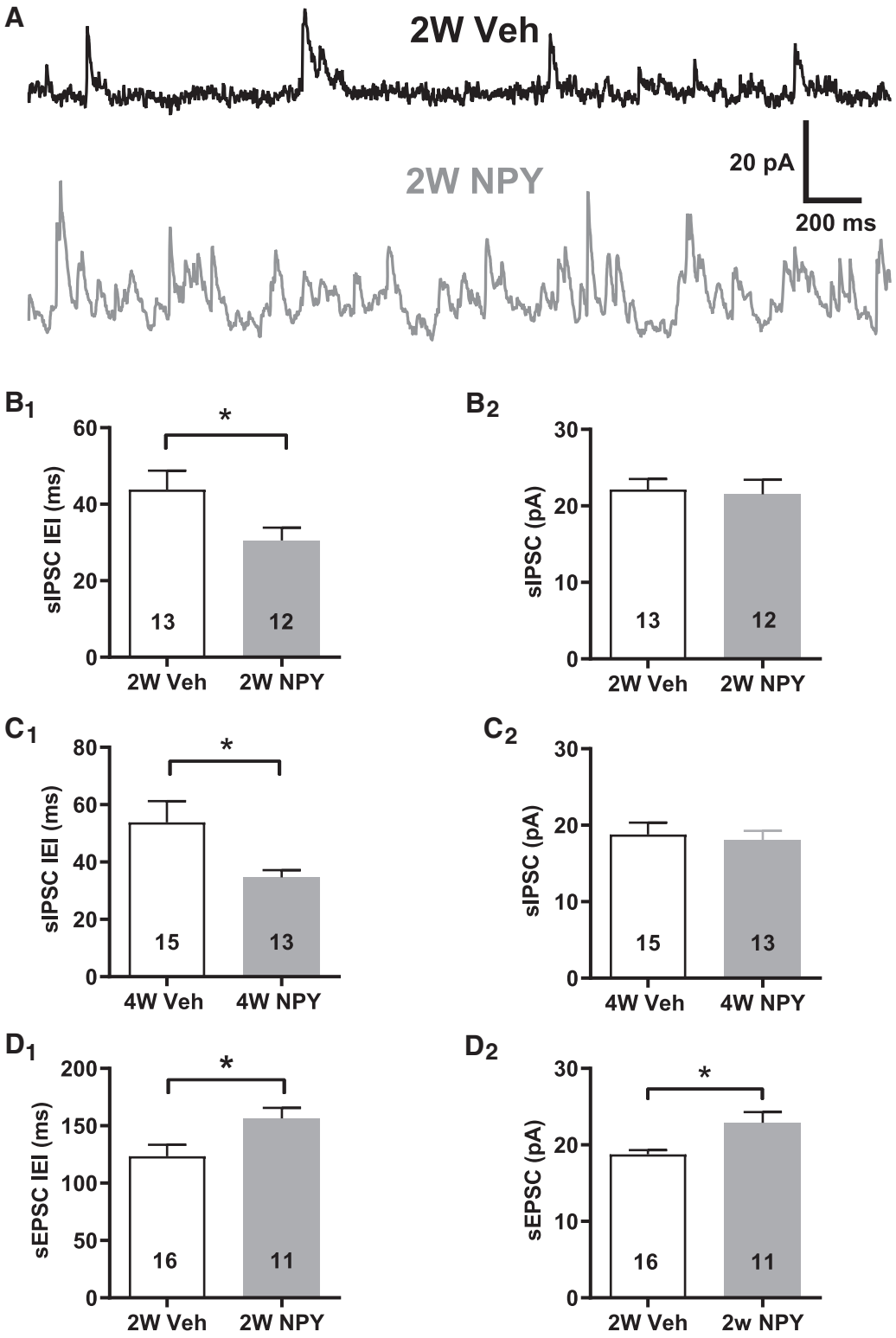

Figure 7. sIPSCs are more frequent in BLA pyramidal cells from 2W and 4W NPY-treated rats. Cs $^{+}$-gluconate recordings, $V_h = -15$ mV. ***A***, Top, sIPSC recording from 2W Veh-treated BLA PN (Lower trace) sIPSC recording from 2W NPY-treated PN. Time and current scale bars as indicated. ***B***, ***B1***, Mean IEI and ***B2***, mean sIPSC amplitude in Cs $^{+}$-gluconate recordings of PNs from 2W Veh- or NPY-treated rats (IEI: $t_{(23)} = 2.19$, $p = 0.039$; amplitude: $t_{(23)} = 0.27$, $p = 0.79$; $n = 12/13$ rats each, 500 events each cell; unpaired *t* test). ***C***, ***C1***, Mean IEI and ***C2***, mean sIPSC amplitude in Cs $^{+}$-gluconate recordings of PNs from 4W Veh- or NPY-treated rats. (IEI: $t_{(26)} = 2.31$, $p = 0.029$; amplitude: $t_{(26)} = 0.36$, $p = 0.73$; $n = 15/13$ rats each, unpaired *t* test). ***D***, ***D1***, Mean IEI and ***D2***, mean sEPSC amplitude in K $^{+}$- gluconate recordings of PNs from 2W Veh- or NPY-treated rats (IEI: $t_{(26)} = 2.44$, $p = 0.022$; amplitude: $t_{(26)} = 2.749$, $p = 0.0166$; $n = 15/11$ rats each, unpaired *t* test). Numbers of neurons tested are indicated in each bar; only a single neuron was recorded from a given animal for these experiments. $^{*}p < 0.05$.

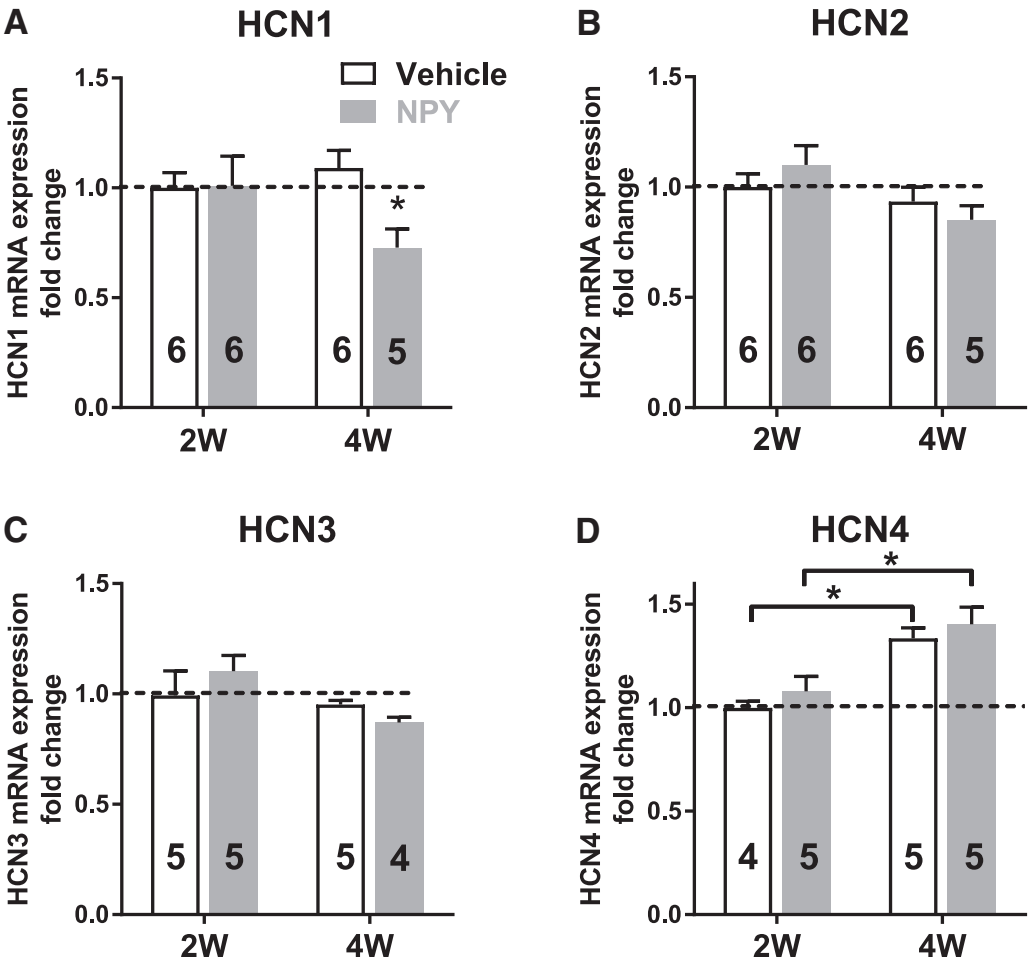

Figure 8. qRT-PCR measurements reveal downregulation of HCN1 expression in 4W NPY- versus 4W Veh-treated BLA. ***A***, HCN1 mRNA expression in 2W and 4W BLA. HCN1 expression was significantly reduced in the BLA of NPY-treated animals at 4W (2-way ANOVA; treatment: $F_{(1,19)} = 4.592, p = 0.04$; *Time:* $F_{(1,19)} = 1.348, p = 0.26$; interaction: $F_{(1,19)} = 5.078, p = 0.03$). ***B***, HCN2 expression in 2W and 4W BLA (2-way ANOVA; treatment: $F_{(1,19)} = 0.229, p = 0.63$; time: $F_{(1,19)} = 2.096, p = 0.164$; interaction: $F_{(1,19)} = 0.345, p = 0.56$). ***C***, HCN3 mRNA in 2W and 4W BLA (2-way ANOVA; treatment: $F_{(1,16)} = 0.84, p = 0.84$; time: $F_{(1,16)} = 3.59, p = 0.08$; interaction: $F_{(1,16)} = 1.73, p = 0.21$). ***D***, HCN4 expression in 2W and 4W BLA. HCN4 expression was increased in 4W relative to 2W BLA in both Veh- and NPY-treated animals, but was not affected by NPY treatment (2-way ANOVA; treatment: $F_{(1,15)} = 1.24, p = 0.28$; time: $F_{(1,15)} = 25.26, p = 0.0002$; interaction: $F_{(1,15)} = 0.0083, p = 0.93$). Data are shown as mean ± SEM; numbers of individual animals studied are indicated in each bar. $^*p < 0.05$, $^{**}p < 0.01$, Bonferroni's multiple-comparisons test; significantly different from 2W time point (Fig. 8*A*) or corresponding 2W group (Fig. 8*D*).

Knock-down of HCN1 expression recapitulates NPY effect on behavior

To examine the contribution of the HCN1 subunit to the generation of long-term increases in SI after repeated NPY treatment, HCN1 subunit expression in the BLA was reduced using a HCN1-shRNA construct in a lentiviral vector (Kim et al., 2012). Placements of the lentivirus injections were located within the BLA, as indicated by the presence of GFP within this region (Fig. 11*A1–A3*); animals with injections outside of the confines of the BLA were not included in the final analysis. Administration of HCN1-shRNA produced a significant (~42%) decrease in the amount of HCN1 protein present in the BLA relative to scr-shRNA (Fig. 11*B1*,*B2*) 4W after injection. In contrast, protein levels of HCN2, the next most abundant isoform, were not affected by the HCN1-shRNA treatment, nor were those of TRIP8b (Fig. 11*B2*). As indicated in Figure 11*C*, SI times started to increase at 1W and reached a maximum at 2W, with levels remaining elevated up to 8W (205.5 ± 33.0%, $F_{(2,14)} = 8.162$, $p = 0.0045$, data not shown).

To assess the effect of HCN1 levels on the expression of stress resilience, animals were subjected to restraint stress and tested for SI at 4W after treatment. An acute 30 min restraint stress produced significant decreases in SI in animals treated with scr-shRNA-treated animals compared with their own baseline values (data not shown) and those of unstressed, scr-shRNA-treated controls (Fig. 11*D*). Treatment with HCN1-shRNA increased SI in the control, unstressed animals at 4W (Fig. 11*C*,*D*). Although restraint stress decreased SI in 4W HCN1-shRNA-treated animals relative to their corresponding nonstress group (Fig. 11*D*), this decrease was modest and SI values were significantly higher than those for the stress scr-shRNA-treated animals (Fig. 11*D*). Therefore, knock-down of HCN1 protein expression in the BLA not only increased SI, but also buffered the effect of restraint stress on SI behavior.

Discussion

Emotional homeostasis requires an appropriate balance between excitation and inhibition within BLA principal output neurons of BLA (Heilig et al., 1994; Britton et al., 2000; Sajdyk et al., 2004). Resilience to stress requires buffering anxiety-related imbalances of excitatory tone. In the BLA, CRF-mediated mechanisms cause an elevation in output, resulting in anxiety-like behaviors and

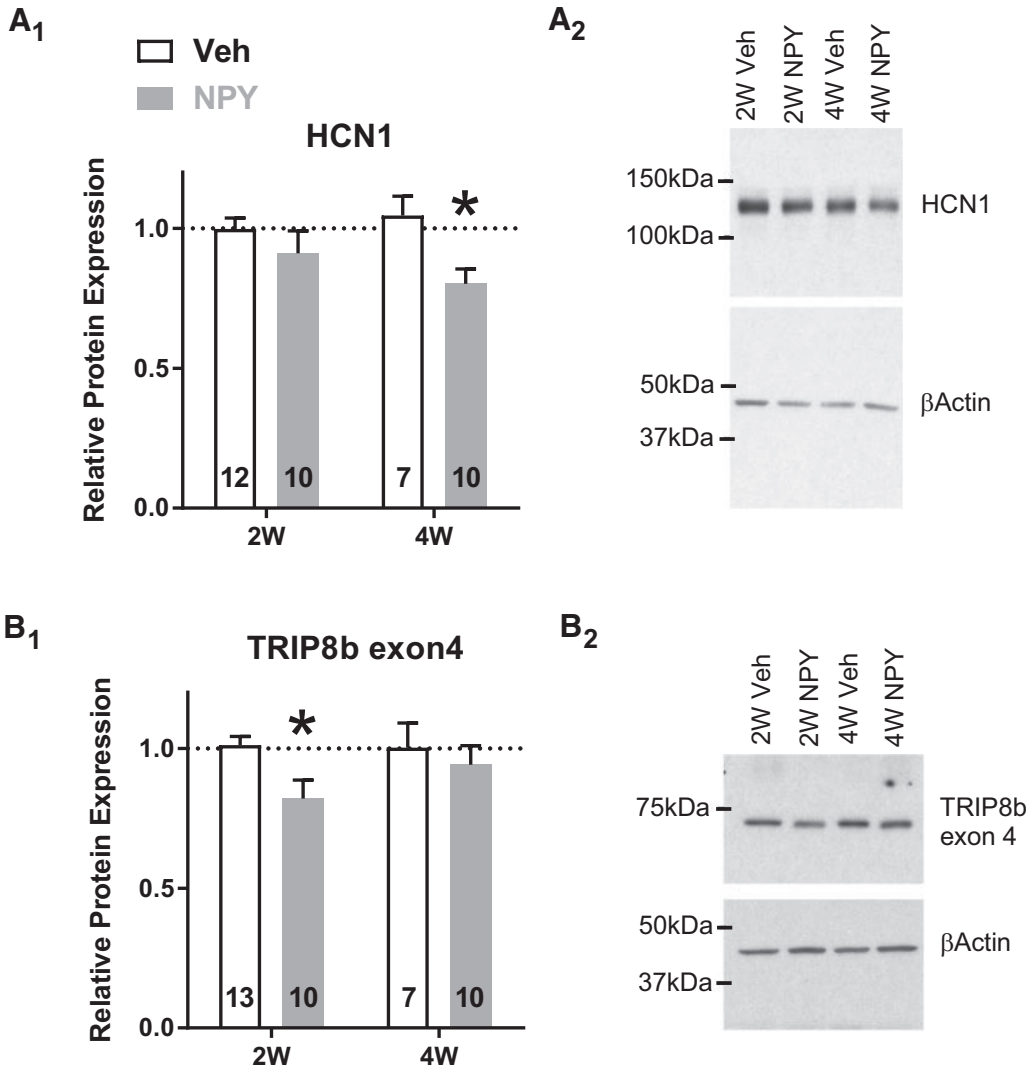

Figure 9. Protein levels of HCN1 and its auxiliary subunit TRIP8b (exon4) are downregulated in BLA tissue from NPY-treated rats. ***A***, Amount of HCN1 protein in the BLA (mean ± SEM) was decreased significantly at 4W, but not 2W, after repeated intra-BLA NPY treatment (2-way ANOVA; treatment: $F_{(1,35)} = 7.22$, $p = 0.011$; time: $F_{(1,35)} = 0.25$, $p = 0.62$; interaction: $F_{(1,35)} = 1.64$, $p = 0.21$). ***B***, Conversely, the protein product of TRIP8b exon 4 (mean ± SEM) was decreased significantly at 2W (2-way ANOVA; treatment: $F_{(1,36)} = 4.23$, $p = 0.047$; time: $F_{(1,36)} = 0.85$, $p = 0.36$; interaction: $F_{(1,36)} = 1.13$, $p = 0.30$). Protein levels were normalized to β-actin as an endogenous control and data are presented relative to W2 Veh. Numbers of animals studied are indicated in each bar. *$p < 0.05$, Bonferroni's multiple-comparisons test.

stress vulnerability (Rainnie et al., 2004; Sajdyk et al., 2004; Truitt et al., 2007; Padival et al., 2013). To maintain a homeostatic balance, an intrinsic mechanism must oppose this imbalance, which likely involves NPY (Heilig et al., 1992, 2004; Morgan et al., 2000; Sajdyk et al., 2008, Giesbrecht et al., 2010; Sah et al., 2014). Although NPY buffers stress acutely, repeated injections of NPY into the BLA induces and models a behavioral stress resilience. Consistent with an anti-stress action of NPY, this repeated NPY treatment reduced the excitability of BLA PNs for at least 4 weeks. Here, we provide evidence that multiple presynaptic and postsynaptic mechanisms interact to reduce BLA excitability and mediate a durable stress resilience.

NPY-induced resilience and I_h

NPY is recognized to buffer anxiety-related behaviors induced by stress and CRF administration. We have demonstrated previously that NPY reduces the activity of BLA PNs acutely by inhibiting resting I_h, causing hyperpolarization and decreased excitability (Giesbrecht et al., 2010). CRF application activates I_h and depolarizes these same cells, suggesting that I_h may represent an "on/off" switch for anxiety, at least in the BLA. Repeated NPY treatment resulted in significant decreases in HCN1 gene and protein expression linked to increases in SI behavior. This reduction in HCN1 protein resulted in a significant, functionally relevant reduction of I_h at 4W after treatment simultaneous with a chronic hyperpolarization of BLA PNs. Interestingly, I_h was not altered in PNs at 2W, nor was HCN1 protein expression reduced, suggesting that other mechanisms mediate PN hyperpolarization at this earlier time point (see below). Nonetheless, the involvement of I_h is likely key to NPY-induced resilience because the knock-down of HCN1 in the BLA also resulted in similar, prolonged increases in SI and buffering of behavioral responses, consistent with an induced resilience to stress.

Although HCN channels are important for neural integration and summation of inputs, there is increasing evidence that these channels are important in modifying behavior. In the hippocampus, knock-down of HCN1 contributes to the generation of antidepressant- and anxiolytic-like behaviors (Kim et al., 2012).

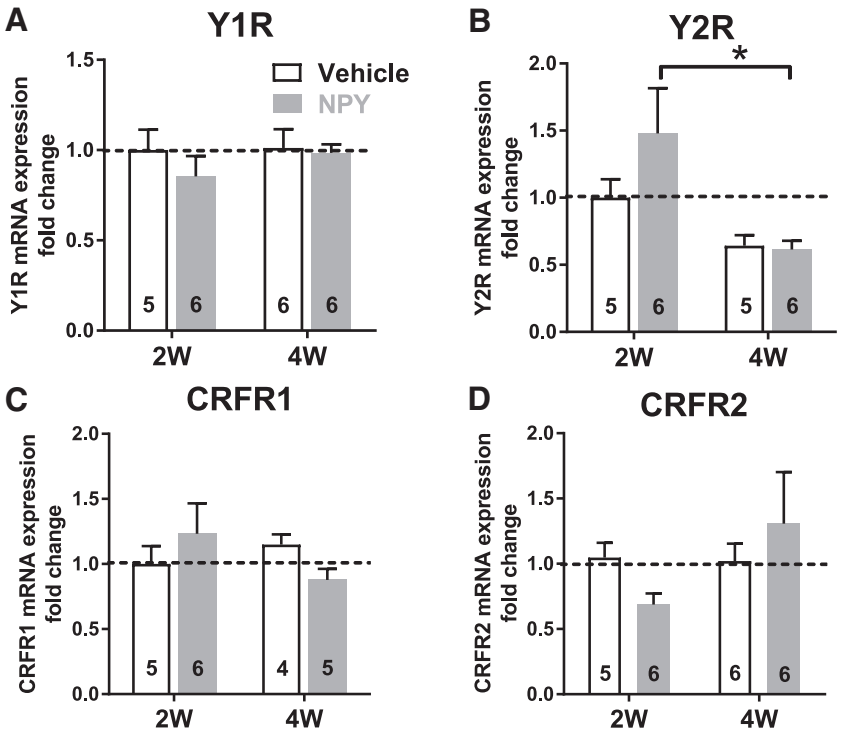

Figure 10. qRT-PCR measurements reveal modulation of NPY_2R expression in BLA. ***A***, Y_1R mRNA from 2W and 4W Veh- and NPY-treated BLA (2-way ANOVA; treatment: $F_{(1,19)} = 0.80$, $p = 0.38$; time: $F_{(1,19)} = 0.53$, $p = 0.48$; interaction: $F_{(1,19)} = 0.37$, $p = 0.55$). ***B***, Y_2R mRNA from 2W and 4W Veh- and NPY-treated BLA. Y_2R mRNA levels are decreased at 4W in the NPY-treated, but not Veh-treated group (2-way ANOVA; treatment: $F_{(1,18)} = 1.24$, $p = 0.28$; time: $F_{(1,18)} = 9.12$, $p = 0.0074$; interaction: $F_{(1,18)} = 1.57$, $p = 0.23$). ***C***, CRFR1 mRNA from 2W and 4W Veh- and NPY-treated BLA (2-way ANOVA; treatment: $F_{(1,16)} = 0.014$, $p = 0.91$; time: $F_{(1,16)} = 0.36$, $p = 0.56$; interaction: $F_{(1,16)} = 2.21$, $p = 0.16$). ***D***, CRFR2 mRNA from 2W and 4W Veh- and NPY-treated BLA (2-way ANOVA; treatment: $F_{(1,19)} = 0.025$, $p = 0.88$; time: $F_{(1,19)} = 1.67$, $p = 0.21$; interaction: $F_{(1,19)} = 1.99$, $p = 0.17$). Numbers of animals studied are represented in each bar. $^*p < 0.05$, Bonferroni's multiple-comparisons test.

The importance of the HCN1 channel subunit to BLA-regulated SIs is demonstrated with the robust increases in SI that accompany shRNA-mediated knock-down of HCN1 protein expression. Although changes in SI behavior are used to assess anxiety (File and Seth, 2003), SI itself is also a rewarding behavior (Douglas et al., 2004). Although NPY has not yet been associated with prosocial behaviors, correlations in the strength of social behaviors and resilience exist and are important in various therapies (Dang, 2014; Neumann and Slattery, 2016). Furthermore, the strong effects of NPY on SI behavior can help add to what is known about the BLA and the regulation of social behaviors. BLA projections to different brain regions (e.g., CeA, BST, NAcc, and mPFC) can be assessed using chemogenetic approaches to determine whether NPY receptor activation targets preferentially the subpopulations of BLA neurons underlying the generation of SI through one or more of these neural circuits.

The decrease of TRIP8b expression observed at 2W suggests a mechanism by which NPY might reduce I_h in BLA PNs. TRIP8b is a chaperone protein that mediates trafficking of HCN1 to the cell surface (Robinson and Siegelbaum, 2003; Santoro et al., 2004; Lewis et al., 2010; Shah, 2014). Although the suppression of TRIP8b prevents HCN1 trafficking, decreases in TRIP8b expression also modestly reduce HCN1 protein expression (Santoro et al., 2004; Lewis et al., 2010, 2011; Piskorowski et al., 2011), perhaps resulting in the reduction in HCN1 expression observed at 4W (Lewis et al., 2009; Santoro et al., 2009). This family of proteins, along with the HCN channel subunits in the hippocampus, have been recent targets for the treatment of depression (Kim et al., 2012, 2018). Our present results suggest that HCN1 and TRIP8b may subserve important roles in the amygdala with respect to stress resilience.

In addition to the NPY-mediated changes both in neuronal excitability and in I_h at 4W, the sensitivity of I_h to the acute actions of either CRF or NPY was also reduced despite stable levels of NPY and CRF receptor gene expression. CRF depolarized BLA PNs modestly at 4W after NPY, suggesting that these neurons can still mount a stress response while losing sensitivity to NPY. Although neither acute (Giesbrecht et al., 2010) nor repeated NPY treatment nor HCN1 knock-down fully eliminated I_h in BLA PNs, I_h reduction seemed sufficient to mediate stress buffering because a significant stressor did not reduce SI time below pretreatment baseline in HCN1-knock-down animals. This further implicates I_h not only as the ultimate target of long-term NPY action on BLA excitability, but also as a means to enhance stress resilience.

HCN channels are prominent on PN dendrites (Berger et al., 2001, 2003; Lewis et al., 2011), where they suppress postsynaptic responses to excitatory input (Tang and Thompson, 2012). Loss of dendritic I_h with repeated NPY exposure will also be expected to increase dendritic input resistance by reducing resting dendritic conductance (Tsay et al., 2007). In turn, increased dendritic resistance should facilitate synaptically mediated depolarizations, whereas the hyperpolarization would promote de-inactivation of dendritic Ca^{2+} channels. Overall, this could sensitize PN dendrites to excitatory synaptic input and facilitate action potential backpropagation and synaptic plasticity (Hamilton et al., 2010). Therefore, whereas NPY actions would largely benefit the animal overall by conferring resilience to minor stressors, these latter changes would still permit it to mount a robust response to stronger adverse stimuli.

Other sequelae of NPY treatment

Although I_h was unaffected at 2W after NPY, the observed persistent increases in spontaneous GABAergic synaptic input could contribute to the hyperpolarization seen in PNs at that time point and this mirrors reports of acute NPY actions in BLA (Berger et al., 2003). The ~20% decrease in sEPSC frequencies might be counterbalanced by the ~20% increase in sEPSC amplitudes, suggesting an at best modest effect via this mechanism at 2W; we did not observe any significant changes in sEPSCs at 4W. Therefore, repeated NPY treatment appears to shift the net balance of synaptic input to BLA PNs toward increased inhibitory tone. Moreover, the reduction of the I_{ir} seen in BLA PNs at 4W NPY would tend to increase their input resistance. Coupled with the relative increase in synaptic inhibition, this might facilitate PN hyperpolarization preferentially. These observations strongly suggest that NPY ultimately invokes an entire suite of complementary inhibitory mechanisms throughout the amygdala (Sosulina et al., 2008).

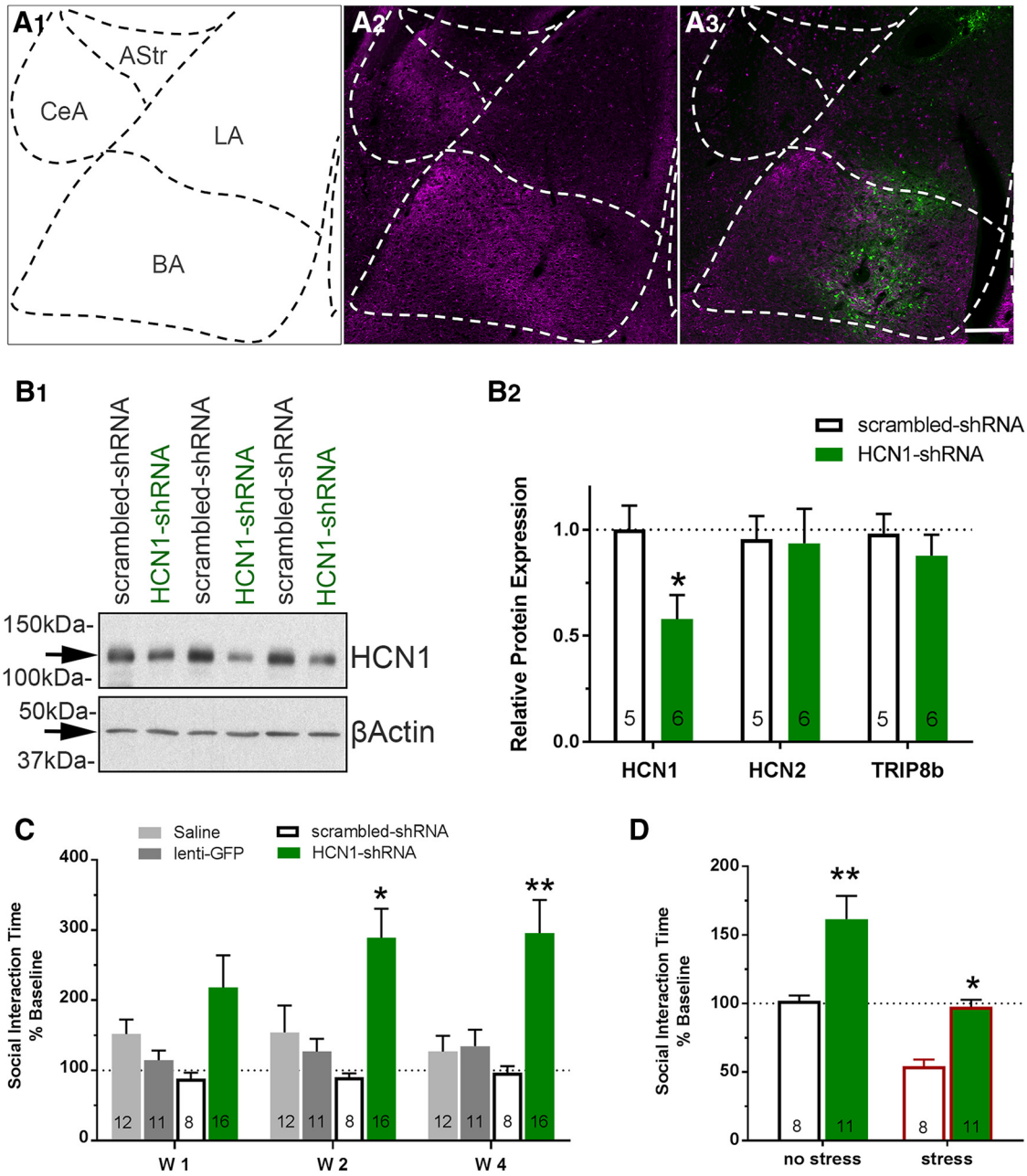

Figure 11. Knock-down of HCN1 in BLA with a lentivirus expressing an HCN1-shRNA construct increases SI times and induces resilience to restraint stress. ***A***, Representative photomicrographs of lentivirus injection sites in the BLA. ***A1***, Schematic representation of the BLA and surrounding structures at −3.30 mm from bregma (adopted from Paxinos and Watson rat brain atlas). ***A2***, ***A3***, Section of BLA showing HCN1 immunoreactivity (magenta; ***A2***) with highest intensities in the BL from a naive uninjected rat and a representative injection placement for HCN1-shRNA (**A3**). Note the green cells indicating transfection (GFP) by the lentivirus. ***B1***, Representative Western blot of HCN1and β-actin protein from the BLA of scr-shRNA- and HCN1-shRNA-injected rats (3 individual samples from each group at 4W after injection). ***B2***, Amount of HCN1 protein was decreased significantly in the BLA of HCN1-shRNA- compared with scr-shRNA-injected rats (unpaired *t* test: $t_{(9)} = 2.61, p = 0.028$), whereas HCN2 (unpaired *t* test: $t_{(9)} = 0.095, p = 0.93$) and TRIP8b (unpaired *t* test: $t_{(9)} = 0.76, p = 0.47$) levels in the BLA were unaffected by the treatment in the same animals. Protein levels were normalized to β-actin as an endogenous control and data are presented relative to scr-shRNA. *N* values are represented in each bar. Scale bar, 100 μm. ***C***, SI time was increased significantly at 2W and 4W after HCN1-shRNA knock-down compared with sh-scrambled injected animals (2-way RM-ANOVA; treatment: $F_{(3,43)} = 6.29, p = 0.0012$; time: $F_{(2,86)} = 1.73, p = 0.18$; interaction: $F_{(6,86)} = 1.92, p = 0.086$, mean ± SEM). ***D***, Restraint stress decreased SI time in both scr-shRNA and HCN1-shRNA-treated animals; however, knock-down of HCN1 prevented the reduction of SI below the respective baseline control values (2-way ANOVA; treatment: $F_{(1,34)} = 28.07, p < 0.0001$; stress: $F_{(1,34)} = 7.95, p = 0.0080$; interaction: $F_{(1,34)} = 0.56, p = 0.46$). Significant differences in poststress SI times were noted between the scr-shRNA and HCN1-shRNA groups. SI time was decreased significantly relative to pretreatment baseline after restraint stress in the scr-shRNA-treated animals (paired *t* test; $t_{(10)} = 4.83, p = 0.0007$), but not in the HCN1-shRNA-treated animals (paired *t* test; $t_{(7)} = 0.29, p = 0.78$). *$p < 0.05$, **$p < 0.01$, ***$p < 0.001$, ****$p < 0.0001$, Bonferroni's multiple-comparisons test or *t* test where appropriate.

Conclusions

Overall, we have identified neuronal mechanisms underlying a robust and physiologically relevant model of emotional homeostasis and behavioral stress resilience. Within the BLA, NPY initiates a complex, coordinated response, resulting in reduced activity in BLA PNs and this could counterbalance at least some long-term changes wrought by persistent stressors. The definitive presence of such a chronic resilience component and the involvement of the HCN1 and TRIP8b proteins within the BLA has been largely absent in the contemplation of stress biology. Future work

must consider the receptors and mechanisms underlying these changes, with the goal of establishing principles by which the state of stress resilience may be induced and maintained.

References

Berger T, Larkum ME, Lüscher HR (2001) High I(h) channel density in the distal apical dendrite of layer V pyramidal cells increases bidirectional attenuation of EPSPs. J Neurophysiol 85:855–868. CrossRef Medline

Berger T, Senn W, Lüscher HR (2003) Hyperpolarization-activated current ih disconnects somatic and dendritic spike initiation zones in layer V pyramidal neurons. J Neurophysiol 90:2428–2437. CrossRef Medline

Britton KT, Akwa Y, Spina MG, Koob GF (2000) Neuropeptide Y blocks anxiogenic-like behavioral action of corticotropin-releasing factor in an operant conflict test and elevated plus maze. Peptides 21:37–44. CrossRef Medline

Broqua P, Wettstein JG, Rocher MN, Gauthier-Martin B, Junien JL (1995) Behavioral effects of neuropeptide Y receptor agonists in the elevated plus-maze and fear-potentiated startle procedures. Behav Pharmacol 6:215–222. Medline

Dang MT (2014) Social connectedness and self-esteem: predictors of resilience in mental health among maltreated homeless youth. Issues Ment Health Nurs 35:212–219. CrossRef Medline

Douglas LA, Varlinskaya EI, Spear LP (2004) Rewarding properties of social interactions in adolescent and adult male and female rats: impact of social versus isolate housing of subjects and partners. Dev Psychobiol 45:153–162. CrossRef Medline

Doupnik CA, Lim NF, Kofuji P, Davidson N, Lester HA (1995) Intrinsic gating properties of a cloned G protein-activated inward rectifier K+ channel. J Gen Physiol 106:1–23. CrossRef Medline

Ekman R, Juhasz P, Heilig M, Agren H, Costello CE (1996) Novel neuropeptide Y processing in human cerebrospinal fluid from depressed patients. Peptides 17:1107–1111. CrossRef Medline

File SE, Seth P (2003) A review of 25 years of the social interaction test. Eur J Pharmacol 463:35–53. CrossRef Medline

Giesbrecht CJ, Mackay JP, Silveira HB, Urban JH, Colmers WF (2010) Countervailing modulation of ih by neuropeptide Y and corticotrophin-releasing factor in basolateral amygdala as a possible mechanism for their effects on stress-related behaviors. J Neurosci 30:16970–16982. CrossRef Medline

Gutman AR, Yang Y, Ressler KJ, Davis M (2008) The role of neuropeptide Y in the expression and extinction of fear-potentiated startle. J Neurosci 28:12682–12690. CrossRef Medline

Hamilton TJ, Wheatley BM, Sinclair DB, Bachmann M, Larkum ME, Colmers WF (2010) Dopamine modulates synaptic plasticity in dendrites of rat and human dentate granule cells. Proc Natl Acad Sci U S A 107:18185–18190. CrossRef Medline

Heilig M, McLeod S, Koob GK, Britton KT (1992) Anxiolytic-like effect of neuropeptide Y (NPY), but not other peptides in an operant conflict test. Regul Pept 41:61–69. CrossRef Medline

Heilig M, Koob GF, Ekman R, Britton KT (1994) Corticotropin-releasing factor and neuropeptide Y: role in emotional integration. Trends Neurosci 17:80–85. CrossRef Medline

Heilig M, Zachrisson O, Thorsell A, Ehnvall A, Mottagui-Tabar S, Sjögren M, Asberg M, Ekman R, Wahlestedt C, Agren H (2004) Decreased cerebrospinal fluid neuropeptide Y (NPY) in patients with treatment refractory unipolar major depression: preliminary evidence for association with preproNPY gene polymorphism. J Psychiatr Res 38:113–121. CrossRef Medline

Horn SR, Charney DS, Feder A (2016) Understanding resilience: new approaches for preventing and treating PTSD. Exp Neurol 284:119–132. CrossRef Medline

Hubert GW, Li C, Rainnie DG, Muly EC (2014) Effects of stress on AMPA receptor distribution and function in the basolateral amygdala. Brain Struct Funct 219:1169–1179. CrossRef Medline

Joëls M, Baram TZ (2009) The neuro-symphony of stress. Nat Rev Neurosci 10:459–466. CrossRef Medline

Kask A, Harro J, von Hörsten S, Redrobe JP, Dumont Y, Quirion R (2002) The neurocircuitry and receptor subtypes mediating anxiolytic-like effects of neuropeptide Y. Neurosci Biobehav Rev 26:259–283. CrossRef Medline

Kim CS, Chang PY, Johnston D (2012) Enhancement of dorsal hippocampal activity by knock-down of HCN1 channels leads to anxiolytic- and antidepressant-like behaviors. Neuron 75:503–516. CrossRef Medline

Kim CS, Brager DH, Johnston D (2018) Perisomatic changes in h-channels regulate depressive behaviors following chronic unpredictable stress. Mol Psychiatry 23:892–903. CrossRef Medline

Lewis AS, Schwartz E, Chan CS, Noam Y, Shin M, Wadman WJ, Surmeier DJ, Baram TZ, Macdonald RL, Chetkovich DM (2009) Alternatively spliced isoforms of TRIP8b differentially control h channel trafficking and function. J Neurosci 29:6250–6265. CrossRef Medline

Lewis AS, Estep CM, Chetkovich DM (2010) The fast and slow ups and downs of HCN channel regulation. Channels (Austin) 4:215–231. CrossRef Medline

Lewis AS, Vaidya SP, Blaiss CA, Liu Z, Stoub TR, Brager DH, Chen X, Bender RA, Estep CM, Popov AB, Kang CE, Van Veldhoven PP, Bayliss DA, Nicholson DA, Powell CM, Johnston D, Chetkovich DM (2011) Deletion of the hyperpolarization-activated cyclic nucleotide-gated channel auxiliary subunit TRIP8b impairs hippocampal ih localization and function and promotes antidepressant behavior in mice. J Neurosci 31:7424–7440. CrossRef Medline

Livak KJ, Schmittgen TD (2001) Analysis of relative gene expression data using real-time quantitative PCR and the 2(-delta delta C(T)) method. Methods 25:402–408. CrossRef Medline

Mirante O, Brandalise F, Bohacek J, Mansuy IM (2014) Distinct molecular components for thalamic- and cortical-dependent plasticity in the lateral amygdala. Front Mol Neurosci 7:62. CrossRef Medline

Morgan CA 3rd, Wang S, Southwick SM, Rasmusson A, Hazlett G, Hauger RL, Charney DS (2000) Plasma neuropeptide-Y concentrations in humans exposed to military survival training. Biol Psychiatry 47:902–909. CrossRef Medline

Neumann ID, Slattery DA (2016) Oxytocin in general anxiety and social fear: a translational approach. Biol Psychiatry 79:213–221. CrossRef Medline

Oken BS, Chamine I, Wakeland W (2015) A systems approach to stress, stressors and resilience in humans. Behav Brain Res 282:144–154. CrossRef Medline

Padival M, Quinette D, Rosenkranz JA (2013) Effects of repeated stress on excitatory drive of basal amygdala neurons in vivo. Neuropsychopharmacology 38:1748–1762. CrossRef Medline

Paxinos G, Watson C (2013) The rat brain in stereotaxic coordinates, Ed 7. New York: Academic.

Piskorowski R, Santoro B, Siegelbaum SA (2011) TRIP8b splice forms act in concert to regulate the localization and expression of HCN1 channels in CA1 pyramidal neurons. Neuron 70:495–509. CrossRef Medline

Rainnie DG, Bergeron R, Sajdyk TJ, Patil M, Gehlert DR, Shekhar A (2004) Corticotrophin releasing factor-induced synaptic plasticity in the amygdala translates stress into emotional disorders. J Neurosci 24:3471–3479. CrossRef Medline

Rasmusson AM, Hauger RL, Morgan CA, Bremner JD, Charney DS, Southwick SM (2000) Low baseline and yohimbine-stimulated plasma neuropeptide Y (NPY) levels in combat-related PTSD. Biol Psychiatry 47:526–539. CrossRef Medline

Robinson RB, Siegelbaum SA (2003) Hyperpolarization-activated cation currents: from molecules to physiological function. Annu Rev Physiol 65:453–480. CrossRef Medline

Sah R, Ekhator NN, Jefferson-Wilson L, Horn PS, Geracioti TD Jr (2014) Cerebrospinal fluid neuropeptide Y in combat veterans with and without posttraumatic stress disorder. Psychoneuroendocrinology 40:277–283. CrossRef Medline

Sajdyk TJ, Shekhar A, Gehlert DR (2004) Interactions between NPY and CRF in the amygdala to regulate emotionality. Neuropeptides 38:225–234. CrossRef Medline

Sajdyk TJ, Johnson PL, Leitermann RJ, Fitz SD, Dietrich A, Morin M, Gehlert DR, Urban JH, Shekhar A (2008) Neuropeptide Y in the amygdala induces long-term resilience to stress-induced reductions in social responses but not hypothalamic-adrenal-pituitary axis activity or hyperthermia. J Neurosci 28:893–903. CrossRef Medline

Santoro B, Wainger BJ, Siegelbaum SA (2004) Regulation of HCN channel surface expression by a novel C-terminal protein-protein interaction. J Neurosci 24:10750–10762. CrossRef Medline

Santoro B, Piskorowski RA, Pian P, Hu L, Liu H, Siegelbaum SA (2009) TRIP8b splice variants form a family of auxiliary subunits that regulate gating and trafficking of HCN channels in the brain. Neuron 62:802–813. CrossRef Medline

Shah MM (2014) Cortical HCN channels: function, trafficking and plasticity. J Physiol 592:2711–2719. CrossRef Medline

Smith BN, Dudek FE (1996) Amino acid-mediated regulation of spontaneous synaptic activity patterns in the rat basolateral amygdala. J Neurophysiol 76:1958–1967. CrossRef Medline

Sosulina L, Schwesig G, Seifert G, Pape HC (2008) Neuropeptide Y activates a G-protein-coupled inwardly rectifying potassium current and dampens excitability in the lateral amygdala. Mol Cell Neurosci 39:491–498. CrossRef Medline

Tang CM, Thompson S (2012) Peturbations of dendritic excitability in epilepsy. In: Jasper's basic mechanisms of the epilepsies (Noebels JL, Avoli M, Rogawski MA, Olsen RW, Delgado-Escueta AV, eds), pp 1–15. Bethesda: National Center for Biotechnology Information.

Truitt WA, Sajdyk TJ, Dietrich AD, Oberlin B, McDougle CJ, Shekhar A (2007) From anxiety to autism: spectrum of abnormal social behaviors modeled by progressive disruption of inhibitory neuronal function in the basolateral amygdala in Wistar rats. Psychopharmacology (Berl) 191: 107–118. CrossRef

Tsay D, Dudman JT, Siegelbaum SA (2007) HCN1 channels constrain synaptically evoked Ca2+ spikes in distal dendrites of CA1 pyramidal neurons. Neuron 56:1076–1089. CrossRef Medline

Ulrich-Lai YM, Herman JP (2009) Neural regulation of endocrine and autonomic stress responses. Nat Rev Neurosci 10:397–409. CrossRef Medline

Vyas A, Mitra R, Shankaranarayana Rao BS, Chattarji S (2002) Chronic stress induces contrasting patterns of dendritic remodeling in hippocampal and amygdaloid neurons. J Neurosci 22:6810–6818. Medline

Vyas A, Jadhav S, Chattarji S (2006) Prolonged behavioral stress enhances synaptic connectivity in the basolateral amygdala. Neuroscience 143:387–393. CrossRef Medline

Yehuda R, Flory JD, Southwick S, Charney DS (2006) Developing an agenda for translational studies of resilience and vulnerability following trauma exposure. Ann N Y Acad Sci 1071:379–396. CrossRef Medline

Zhou Z, Zhu G, Hariri AR, Enoch MA, Scott D, Sinha R, Virkkunen M, Mash DC, Lipsky RH, Hu XZ, Hodgkinson CA, Xu K, Buzas B, Yuan Q, Shen PH, Ferrell RE, Manuck SB, Brown SM, Hauger RL, Stohler CS (2008) Genetic variation in human NPY expression affects stress response and emotion. Nature 452:997–1001. CrossRef Medline

Zuj DV, Palmer MA, Lommen MJ, Felmingham KL (2016) The centrality of fear extinction in linking risk factors to PTSD: a narrative review. Neurosci Biobehav Rev 69:15–35. CrossRef Medline